

Design of a Dual Polarized Slot Antenna in MLW Technology

The design of a slot antenna that supports two orthogonal polarizations, radiated by the same waveguide structure that supports two modes in MLW technology.

Master's thesis in Wireless, Photonics and Space Engineering

Sergio Alejandro Carrasco Paz

DEPARTMENT OF SOME SUBJECT OR TECHNOLOGY

CHALMERS UNIVERSITY OF TECHNOLOGY
Gothenburg, Sweden 2024
www.chalmers.se

MASTER'S THESIS 2024

Design of a Dual Polarized Slot Antenna in MLW Technology

The design of a slot antenna that supports two orthogonal polarizations, radiated by the same waveguide structure that supports two modes in MLW technology.

Sergio Alejandro Carrasco Paz



CHALMERS
UNIVERSITY OF TECHNOLOGY

Department of Electrical Engineering
Antenna System Group
CHALMERS UNIVERSITY OF TECHNOLOGY
Gothenburg, Sweden 2024

Design of a Dual Polarized Slot Antenna in MLW Technology

The design of a slot antenna that supports two orthogonal polarizations, radiated by the same waveguide structure that supports two modes in MLW technology.

Sergio Alejandro Carrasco Paz

© Sergio Alejandro Carrasco Paz, 2024.

Supervisor: Coen van de Ven, GAPWAVES

Examiner: Professor Jian Yang, Department of Antenna Systems

Master's Thesis 2024

Department of Electrical Engineering

Antenna System Group

Chalmers University of Technology

SE-412 96 Gothenburg

Telephone +46 31 772 1000

Cover: Slot antenna design constructed in CST.

Typeset in L^AT_EX

Printed by Chalmers Reproservice

Gothenburg, Sweden 2024

Design of a Dual Polarized Slot Antenna in MLW Technology

The design of a slot antenna that supports two orthogonal polarizations, radiated by the same waveguide structure that supports two modes in MLW technology.

Sergio Alejandro Carrasco Paz

Department of Electrical Engineering

Chalmers University of Technology

Abstract

In the fifth-generation cellular networks, frequency bands have been allocated in the mmWave regime to take advantage of the large bandwidth at these frequencies. To take full advantage of this bandwidth, spectral efficiency should be increased as much as possible. One of the ways to increase spectral efficiency is by exploiting diversity. Diversity can be created in several ways, for example by using multiple antenna in a MIMO system. Besides this, polarization diversity has been deployed at lower frequencies, however this becomes a challenge at mmWave, since the antenna system needs to be able to radiate two orthogonal polarizations. Together with the half wavelength spacing of a typical MIMO-array the waveguide should support two modes to keep the polarizations sufficiently isolated.

Another challenge at mmWave frequencies are the dielectric losses associated with the printed circuit board. To avoid these losses, waveguide antennas can be used which have lower losses. Traditionally, waveguide antennas are difficult to be manufactured since they need galvanic contact between the different layers of the antenna. Gapwaveguide technology removes this problem with the use of EBG structures, which can tolerate a gap between the different layers of the mechanical assembly. Moreover, the new MLW technology allows for an even smaller form factor and allows for smaller structures in its layers, which opens up design space.

Therefore, this project aims to create a dual polarized antenna element in MLW technology at 66-71 GHz, (the upper half of the 5G NR n263 frequency band). The antenna element is aimed to support two modes in the same waveguide structure which radiate in two orthogonal polarizations. Furthermore, the antenna shall have a number of radiating slots along the waveguide to investigate the potential impact of grating lobes.

Keywords: MLW, Slot, Antenna, Dual-Polarized, gap-waveguide.

Acknowledgements

Lorem ipsum dolor sit amet, consectetur adipiscing elit, sed do eiusmod tempor incididunt ut labore et dolore magna aliqua. Ut enim ad minim veniam, quis nostrud exercitation ullamco laboris nisi ut aliquip ex ea commodo consequat. Duis aute irure dolor in reprehenderit in voluptate velit esse cillum dolore eu fugiat nulla pariatur. Excepteur sint occaecat cupidatat non proident, sunt in culpa qui officia deserunt mollit anim id est laborum.

Sergio Alejandro Carrasco Paz, Gothenburg, June 2024

List of Acronyms

Below is the list of acronyms that have been used throughout this thesis listed in alphabetical order:

MLW	Multilayer Waveguide
EBG	Electromagnetic Band-Gap
EM	Electromagnetic
LHC	Left-Hand Circular
RHC	Right-Hand Circular

Nomenclature

Below is the nomenclature of indices, sets, parameters, and variables that have been used throughout this thesis.

Indices



Contents

List of Acronyms	ix
Nomenclature	xi
List of Figures	xv
List of Tables	xix
1 Introduction	1
1.1 Aim and Goals	1
1.2 Outline of Thesis	1
2 Theory	3
2.1 Electromagnetic Theory	3
2.1.1 Maxwell Equations	3
2.1.2 Plane Waves	4
2.1.2.1 Polarization	5
2.2 Transmission Line Theory	6
2.3 Waveguides	7
2.3.1 Microstrip line	7
2.3.2 Coupled Microstrip Line	8
2.4 Gap Waveguide	10
2.5 Multilayer Waveguide	12
2.6 Antenna Theory	13
2.6.1 Antenna Parameters	13
2.6.2 Slot Antenna	14
3 Design	17
3.1 Waveguide Restrictions	17
3.1.1 Waveguide Design	20
3.2 MLW Restrictions	20
3.2.1 Mode Selection	21
3.2.2 MLW Design	23
3.3 Antenna Design	24
3.3.1 Extra Elements for the horizontal slot	27
3.3.2 Slot excitation	30
3.3.3 Horn	31

4	Results	33
4.1	MLW Results	33
4.2	Slot results	34
4.3	Operation	35
5	Discussion	41
5.1	Performance	41
5.2	Slot	41
5.3	Future work	42
5.4	Conclusion	42
	Bibliography	43

List of Figures

2.1	Forward uniform plane wave [1]	5
2.2	Microstrip line [5]	8
2.3	Microstrip line in an homogeneous medium [5]	8
2.4	Coupled stripline [5]	9
2.5	Coupled stripline [5]	9
2.6	Even Mode Excitation[5]	9
2.7	Equivalent Circuit[5]	9
2.8	Odd Mode Excitation[5]	10
2.9	Equivalent Circuit[5]	10
2.10	Cross section of ideal gap waveguide [9]	10
2.11	Bed of Pins surrounding a feeding ridge [9]	11
2.12	Dispersion Diagrams of the first 30 modes a) All modes plotted indistinctly b) Desired modes marked c) Undesired mode marked d) Stop band	12
2.13	Gap waveguide geometries and their desired modes of propagation[9]	12
2.14	Cross-sectional view of an MLW transmission line with field-leakage suppression[11]	13
2.15	Polar plot of a radiation pattern, showing Gain and Side-lobes of an antenna (red) against the radiation pattern of an isotropic antenna (green)	14
3.1	Even (left) and Odd (right) modes simulation in CST	18
3.2	Dimensions nomenclature for the microstrip approximation	19
3.3	Normalized even- and odd-mode characteristic impedance design data for symmetric edge-coupled striplines [5]	19
3.4	Transmission efficiency for each mode dependant of distance between the slot and the short circuit	20
3.5	Expanded view of the MLW proposed in [10]	21
3.6	Geometry of the EBG unit cell	21
3.7	Dispersion diagram for the infinite periodic EBG unit cell($Face = 1.1mm$, $Period = 2.2mm$)	22
3.8	Dispersion diagram for the stopband of an infinite periodic EBG unit cell raging from $Face = 0.8mm$, $Period = 1.6mm$ to $Face = 1.2mm$, $Period = 2.4mm$	22
3.9	Transversal view of the waveguide	23
3.10	Dispersion diagram of the periodic transversal section of the MLW	23

3.11	Dispersion diagram of the periodic transversal section of the MLW for different widths of the channel ($1.5mm, 1.6mm, 1.7mm, 1.8mm, 1.9mm, 2mm$)	24
3.12	Admittance of the even mode (upper) and odd mode (lower) of a single slot	24
3.13	Schematic view of the antenna element tripole slots[4]	25
3.14	Excitation of the waveguide slots by the even mode on the left, and odd mode on the right[4]	26
3.15	Excitation of the tripole slot with the even mode on the left, and odd mode on the right	26
3.16	Main parameters for the tripole slot	27
3.17	Effect of the Vertical slot Width on the Frequency and admittance a) Impact of Width Variation on Admittance and Frequency for the even mode b) Impact of Width Variation on Admittance and Frequency for the odd mode c) Admittance vs. Frequency of the even mode for Various Widths d) Admittance vs. Frequency of the odd mode for Various Widths	27
3.18	Effect of the Horizontal slot Width on the Frequency and admittance a) Impact of Width Variation on Admittance and Frequency for the even mode b) Impact of Width Variation on Admittance and Frequency for the odd mode c) Admittance vs. Frequency of the even mode for Various Widths d) Admittance vs. Frequency of the odd mode for Various Widths	28
3.19	Effect of the Vertical slot Length on the Frequency and admittance a) Impact of Length Variation on Admittance and Frequency for the even mode b) Impact of Length Variation on Admittance and Frequency for the odd mode c) Admittance vs. Frequency of the even mode for Various Lengths d) Admittance vs. Frequency of the odd mode for Various Lengths	28
3.20	Effect of the Horizontal slot Length on the Frequency and admittance a) Impact of Length Variation on Admittance and Frequency for the even mode b) Impact of Length Variation on Admittance and Frequency for the odd mode c) Admittance vs. Frequency of the even mode for Various Lengths d) Admittance vs. Frequency of the odd mode for Various Lengths	29
3.21	Effect of the Angle on the Frequency and admittance a) Impact of Angle Variation on Admittance and Frequency for the even mode b) Impact of Angle Variation on Admittance and Frequency for the odd mode c) Admittance vs. Frequency of the even mode for Various Angles d) Admittance vs. Frequency of the odd mode for Various Angles	29
3.22	Initial Slot model on the left, and model with dumbbells on the right	30
3.23	Electric field propagation in the horizontal slot, initial slot on the left, and slot with dumbbells on the right	30
3.24	Comparison between the S_{11} parameter of the Even mode (left) and Odd mode (right), with $0.2mm$ dumbbells (green) and without (red)	30
3.25	Feeding line bent to improve slot excitation	31

3.26	Feeding line bent comparison from 73° to 90°	31
3.27	Effect of the Bent Lines on the Frequency and admittance a) Impact of Bent Lines on Admittance and Frequency for the even mode b) Impact of Bent Lines on Admittance and Frequency for the odd mode c) Admittance vs. Frequency of the even mode for Various Lengths d) Admittance vs. Frequency of the odd mode for Various Lengths . .	32
4.1	Approximated dimensions for the MLW design	33
4.2	Slot design with dumbbells delimited by proximity to the side pins . .	34
4.3	Final slot design	34
4.4	Dimensions of the final slot	35
4.5	S_{11} Parameter Against Frequency of the even mode	36
4.6	S_{11} Parameter Against Frequency of the even mode	36
4.7	Even mode Elevation Radiation pattern of one slot antenna a)With Horn b) Without Horn	36
4.8	Odd mode Azimuth Radiation pattern of one slot antenna a)With Horn b) Without Horn	37
4.9	3 Slots model	37
4.10	Even mode Radiation pattern of three slots with horn a)Azimuth b)Elevation	38
4.11	Odd mode Radiation pattern of three slots with horn a)Azimuth b)Elevation	39

List of Tables

2.1	Unit vector for polarizations	6
3.1	Specifications benchmark	18

1

Introduction

This chapter presents the section levels that can be used in the template.

1.1 Aim and Goals

The aim of this thesis is to create a dual polarized antenna element in MLW technology that can work between 66 GHz and 71 GHz. This antenna must be designed for two linear polarizations, feeded and controlled by two orthogonal modes in the same waveguide.

1.2 Outline of Thesis

The following chapters are divided as follows, chapter 2 provides an extensive background on the theory so that the design of the MLW antenna can be understood. Chapter 3 presents the methods used to arrive to the final model, its results are presented in chapter 4. In chapter 5 the results are discussed, highlighting the advantages and disadvantages of the model and future work.

2

Theory

This chapter aims to provide a fundamental understanding of the behavior of electromagnetic waves and different concepts regarding antenna theory. This understanding is crucial for the following chapters up to the conclusion of the thesis.

2.1 Electromagnetic Theory

This chapter provides a basic explanation of the behavior of electromagnetic waves.

2.1.1 Maxwell Equations

Understanding any electromagnetic phenomena starts with Maxwell's equations. This set of four equations describes the behaviour of every electromagnetic event.

$$\begin{aligned}\nabla \times E &= -\frac{\delta B}{\delta t} \\ \nabla \times H &= J + \frac{\delta D}{\delta t} \\ \nabla \cdot D &= \rho \\ \nabla \cdot B &= 0\end{aligned}\tag{2.1}$$

Where E is the electric field, H the magnetic field, D is the electric flux density and B the magnetic flux density. These four equations describe the fundamental laws: Faraday's law of induction, Ampere's law of electromagnetism and Gauss's laws of electricity and magnetism.

Faraday's Law express that a magnetic field that varies in time, will create an electric field, and is the first equation in 2.1

Ampere's law states that magnetic fields can be generated by electric currents, described by the second equation in 2.1

Gauss's law states that the electric flux in a closed surface is proportional to the total charge within the same surface. Analogue to the electric charges, the magnetic flux of any enclosed surface is 0.

Furthermore we can relate $D = \epsilon E$ and $B = \mu H$, where ϵ is the permittivity of the material which indicates how electric fields propagate in a material. μ on the other hand, represents the permeability of the material and relates how magnetic fields propagate in it.

2.1.2 Plane Waves

To continue the analysis of EM fields, it is important to describe them as solutions of Maxwell equations. The easiest and more convenient way to analyze this fields is to start by describing the simplest electromagnetic wave, which is far from the source, in the form of a plane wave. Assuming a Cartesian coordinate system, this waves propagate in one direction (let's say the z -direction) in vacuum. This assumptions means that the wave won't interact with its environment and is independent on the transverse coordinates x or y , making it a function of z and t only.

$$\begin{aligned}\nabla &= \hat{z} \frac{\delta}{\delta z} \\ \nabla \cdot E &= \frac{\delta E_z}{\delta z} \\ \nabla \times E &= -\hat{x} \frac{\delta E_y}{\delta z} + \hat{y} \frac{\delta E_x}{\delta z}\end{aligned}\tag{2.2}$$

Using the simplified forms of the ∇ operator [2.2], and being a function of z and t , allows to equate partial derivatives to 0, ($\delta_x = 0$ and $\delta_y = 0$) and reduce Maxwell's equations to the following:

$$\begin{aligned}z \times \frac{\delta E}{\delta z} &= \mu \frac{\delta H}{\delta t} \\ z \times \frac{\delta H}{\delta z} &= \epsilon \frac{\delta E}{\delta t}\end{aligned}\tag{2.3}$$

$$\begin{aligned}\frac{\delta E_z}{\delta z} &= 0 \\ \frac{\delta H_z}{\delta z} &= 0\end{aligned}$$

This equations describe the wave as constant in the z direction, changing only in the transverse fields. Since the wave is propagating in the z -direction, we can represent the magnetic and electric fields as:

$$\begin{aligned}E(z, t) &= E(z) e^{j\omega t} \\ H(z, t) &= H(z) e^{j\omega t}\end{aligned}\tag{2.4}$$

Where $E(z)$ and $H(z)$ are transverse with each other and can be solved with solutions of forward and backward waves as follows:

$$\begin{aligned} E(z) &= E_{0+} e^{-jkz} (\text{forward}) \\ E(z) &= E_{0-} e^{+jkz} (\text{backward}) \end{aligned} \quad (2.5)$$

Where k is a constant known as the wave number and is defined as the propagation constant of the medium $k = w\sqrt{\mu\epsilon}$.

The solution to these equations as a general solution for a single-frequency wave, can be represented as a superposition of forward and backward components, a time-varying wave depicted in Figure 2.1 and described by equation 2.6.

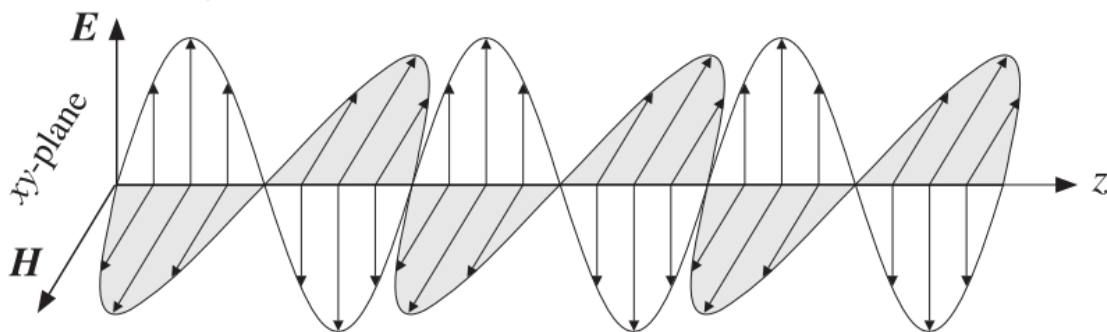


Figure 2.1: Forward uniform plane wave [1]

$$E(z, t) = (\hat{x}A_+ + \hat{y}B_+)e^{(j\omega t - jkz)} \quad (2.6)$$

2.1.2.1 Polarization

Polarization refers to the direction of the electric or magnetic field at any fixed time in space. It can be in a linear, circular or elliptical.[3] This property allows different signals to be modulated on the same carrier, effectively doubling the capacity without interference or degradation.

For example, in equation 2.6, if $B_+ = 0$, the E-field is along the x-direction only, resulting in linear polarization. The polarization is determined by the E-field direction and can be described as the co-polar component (E_{co}) or cross-polar component (E_{xp}), both orthogonal to the propagation direction. Is possible to rewrite equation 2.6 as follows:

$$E = (E_c o \widehat{co} + E_x p \widehat{xp}) e^{(j\omega t)} \quad (2.7)$$

Depending on the values of the unit vectors \widehat{co} and \widehat{xp} , the polarization may be linear, circular or elliptical. For each case, the unit vectors must satisfy the following conditions:

$$\begin{aligned} \widehat{co} &= \cos\xi \widehat{x} + \sin\xi \widehat{y} \\ \widehat{xp} &= \sin\xi \widehat{x} - \cos\xi \widehat{y} \end{aligned} \quad (2.8)$$

The quality of the polarization is given by how good the condition in table 2.1 is satisfied. Elliptical polarization is a combination between both conditions.

Polarization	Linear	Circular
\widehat{co}	\widehat{x}	$\widehat{x} \pm j\widehat{y}/\sqrt{2}$
\widehat{xp}	$-\widehat{y}$	$\widehat{x} \pm j\widehat{y}/\sqrt{2}$

Table 2.1: Unit vector for polarizations

Various factors can cause changes in the polarization like reflection and refraction at the boundary between different media or interaction with objects that can scatter EM waves.

2.2 Transmission Line Theory

Transmission line theory is a fundamental concept in electrical engineering that bridges the gap between field analysis and circuit theory describing the behaviour of signals as they propagate on a transmission line.[5] A transmission line is a network where voltages (V) and currents (I) can vary in magnitude and phase over its length. [5]

A transmission line have at least two conductors (typically wires or printed circuit board) separated by a dielectric material. The changes between voltage and current along its length are described by the telegrapher equations (2.9).

$$\begin{aligned} \frac{\delta V(z, t)}{\delta z} &= -(R + j\omega L)I(z) \\ \frac{\delta I(z, t)}{\delta z} &= -(G + j\omega C)V(z) \end{aligned} \quad (2.9)$$

Where R is the resistance per unit length Ω/m , L is the inductance per unit length in H/m , G is the conductance per unit length S/m and C is the capacitance per unit length F/m .

When a signal is applied in one end of the transmission line, it propagates along the line at a certain velocity ($v = \frac{1}{\sqrt{LC}}$) that is determined by the transmission line parameters.

2.3 Waveguides

A waveguide is a structure that confines and guides an electromagnetic wave along a path, unlike transmission lines which carry signals through conductors, they have the advantage of high power-handling and low loss, especially at low frequencies.[5] Waveguides come in various shapes and forms, each type has its own set of propagation characteristics, and they come with their advantages and disadvantages, it is important to select accordingly to the application.

The shape and design of the waveguide will define the type of waves that can propagate in it. Transverse electromagnetic (TEM) waves are characterized by $E_z = H_z = 0$, they require at least two conductors, and have a lossless dielectric and they have the advantage of travelling through the medium at same velocity, avoiding phase shift. [6][5]

If one of the fields is not equal to 0 ($E_z \neq 0$ or $H_z \neq 0$) the wave will be a transverse electric (TE) or transverse magnetic (TM) wave. Not having one of the fields equal to 0, means that the fields won't be uniform and the presence of either field will affect the distribution inside the waveguide, leading to different undesired electric or magnetic fields.[6][5]

2.3.1 Microstrip line

A microstrip line consists of a conductor of width W on a dielectric substrate (relative permittivity ϵ_r) of thickness d from the ground plane as shown in figure 2.2

This line has the disadvantage of a phase-mismatching between the substrate and air due to differences in permittivity (ϵ_r) makes it impossible to have a TEM wave. To avoid this inconvenience, it is possible to use an equivalent geometry with an homogeneous medium as shown in figure 2.3.

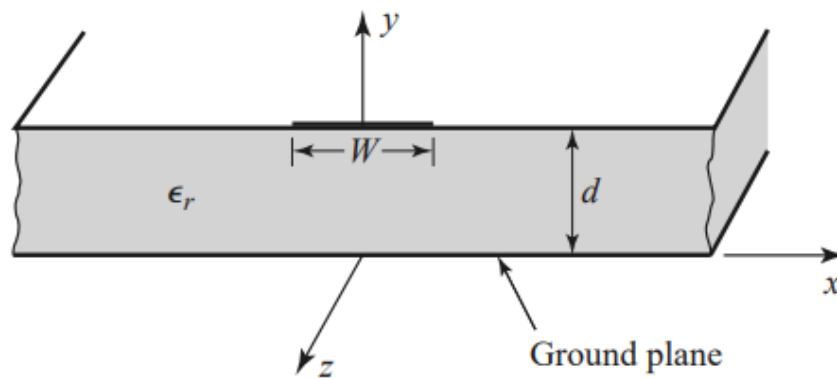


Figure 2.2: Microstrip line [5]

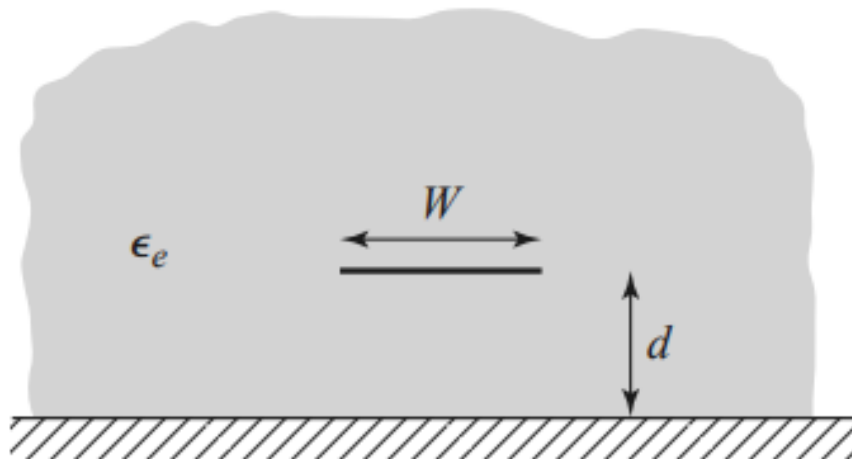


Figure 2.3: Microstrip line in an homogeneous medium [5]

2.3.2 Coupled Microstrip Line

Coupled theory allows to use passive microwave components to accept two or more input signals, and combine them at an output port, this reduces the necessary space for transmission of several signals and led to the development of coupled line directional couplers.

A coupler is characterized by its coupling factor, which is a ratio of the magnetic flux generated by one line that is linked to a second line, this lines will be called "coupled transmission lines" [5][8]. This ratio can range between 0 and 1. They are assumed to work on TEM modes and they can support two distinct propagation modes.

Usually it is desired for the lines to be symmetric as it simplifies the analysis to only the width of the lines, the distance between the lines and the distance between the ground planes as shown in figure 2.4.

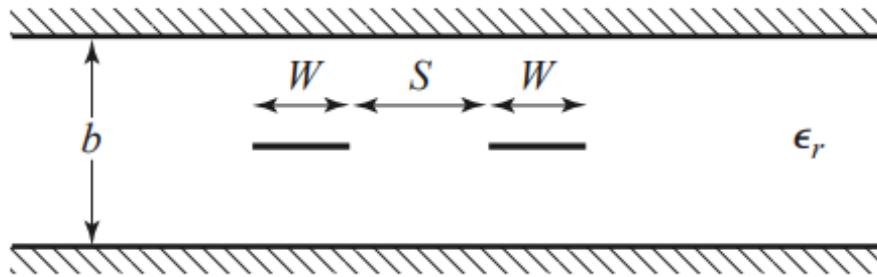


Figure 2.4: Coupled stripline [5]

To analyse the coupled lines, it is possible to represent them as an equivalent circuit of only capacitance, shown in figure 2.5. Where C_{12} represents the capacitance between the two lines, and $C_{11} = C_{22}$ as they are symmetric and represent the capacitance between one line and the ground plane.

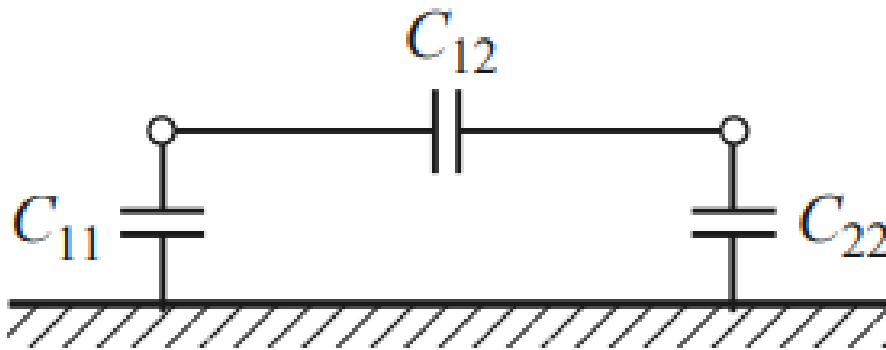


Figure 2.5: Coupled stripline [5]

To do the analysis of the coupled lines, it is important to take into account how the lines are being excited, For two coupled lines, there are two different ways called even and odd mode. In both cases the current amplitude is the same, the direction is the same for even mode but for odd mode the direction is the opposite causing the electromagnetic fields to interact differently and leading to a distinct set of characteristics impedance for each mode although they have the same propagation constant and phase velocity because the line is TEM.

In the even case, the symmetry causes no current flow between the two lines as

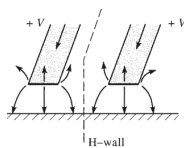


Figure 2.6: Even Mode Excitation[5]



Figure 2.7: Equivalent Circuit[5]

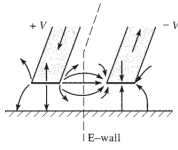


Figure 2.8: Odd Mode Excitation[5]

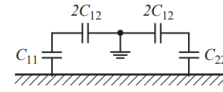


Figure 2.9: Equivalent Circuit[5]

sketch in figure 2.6, making the equivalent circuit to be open as shown in figure 2.7, causing the capacitance to be $C_e = C_{11} = C_{22}$ and resulting in a characteristic impedance of:

$$Z_0 = \sqrt{\frac{L}{C}} = \frac{1}{v_p C} \quad (2.10)$$

For the odd case the symmetry and direction of the current will make the middle to act as a ground plane (Figure 2.8), altering the equivalent circuit as shown in figure 2.9. Resulting in the equivalent capacitance to be $C_o = C_{11} + 2C_{12} = C_{22} + 2C_{12}$, altering the characteristic impedance in equation 2.10.

2.4 Gap Waveguide

Ideal gap waveguides uses the configuration of a parallel plate waveguide to control the propagation between two perfect electrical conductors (PEC), by using a metal plate on one side and a small metal strip line on the other side as shown in Figure 2.10 is possible to propagate EM waves that will only follow the strip.

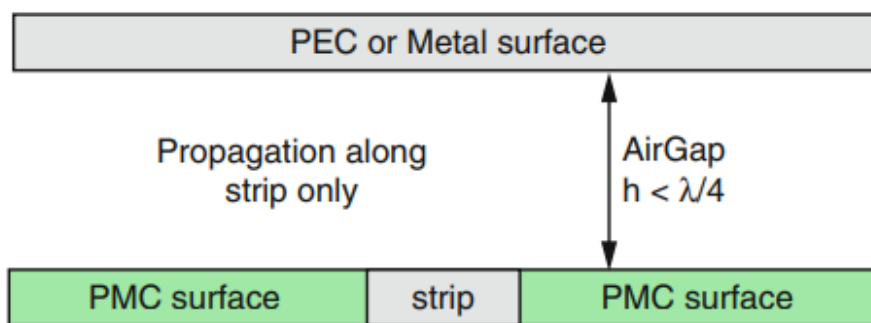


Figure 2.10: Cross section of ideal gap waveguide [9]

To avoid the propagation of the EM wave outside the small strip line, is important to simulate a perfect magnetic conductor (PMC)[9]. The way to do it is by using a periodic structure that will emulate an artificial magnetic conductor (AMC) [9]. This structure will create a stopband that blocks electromagnetic waves of certain frequency bands, also known as an Electromagnetic band-gap (EBG).

This periodic structure will act as a surface impedance that won't allow any modes to propagate, working as a stop band preventing any lateral field leakage into adjacent structures or free space. As long as the gap between the top layer and the lower layer is not bigger than $\lambda/4$, it won't require metal contact between the top layer and the lower surface, this lowers manufacturing cost and simplifies mass production.

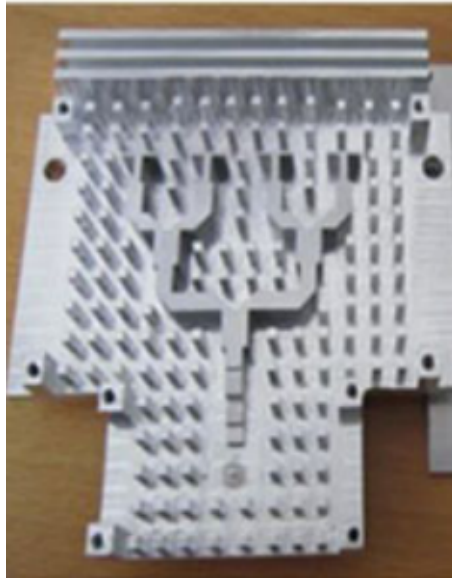


Figure 2.11: Bed of Pins surrounding a feeding ridge [9]

There exist different possible periodic structures, one of the easiest to use is a bed of pins[9], shown in figure 2.11, which must have an air gap smaller than $\lambda/4$. The most important thing when designing the structure is to obtain the lower and upper cutoff frequency that are dependant of the geometrical parameters of the structure. This cut off frequencies will create a space where only the desired mode can propagate as seen in figure 2.12-a).

The objective when designing the periodic structure, is to allow only the desired modes to propagate (Fig. 2.12-b)) in between the stop bands, while maintaining the undesired modes (Fig. 2.12-c)) out of the desired cut off frequencies (Fig. 2.12-d)).

There exist different gap waveguide geometries than can be selected depending of the desired structure, this extend from ridge gap waveguides, groove gap waveguides, and microstrip gap waveguides (Fig.2.13) which can be selected depending on their application.

From the gap waveguide geometries, the ridge gap waveguide can be realized without dielectrics, making it advantageous to microstrip geometries[7], and the desired mode is a Quasi-TEM mode. On the other hand, groove gap waveguides work similar to a TE mode of a rectangular waveguide [9].

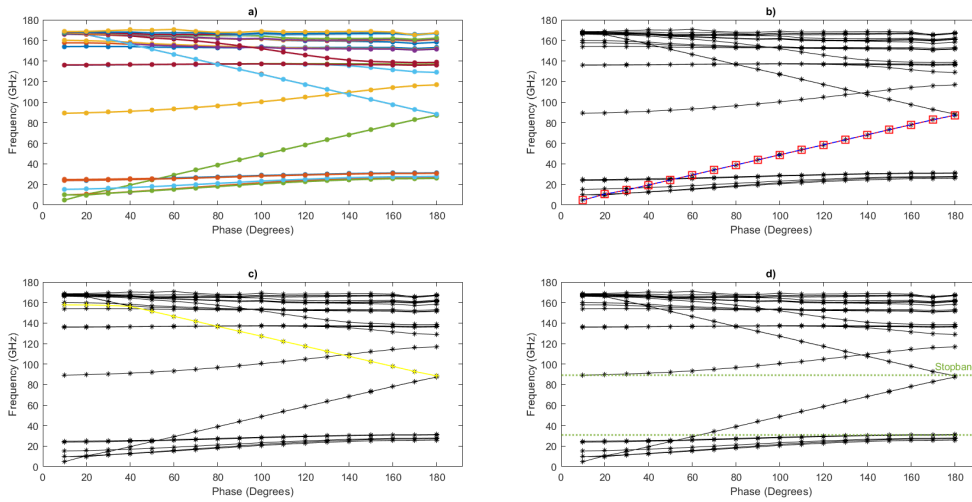


Figure 2.12: Dispersion Diagrams of the first 30 modes a) All modes plotted indistinctly b) Desired modes marked c) Undesired mode marked d) Stop band

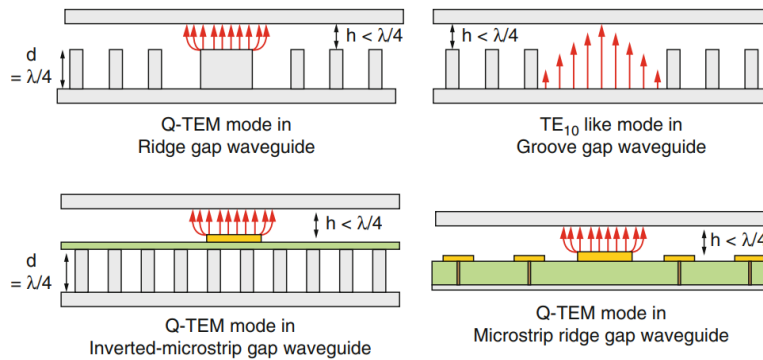


Figure 2.13: Gap waveguide geometries and their desired modes of propagation[9]

2.5 Multilayer Waveguide

Multilayer Waveguide (MLW), is a low-loss air filled coaxial waveguide transmission line, formed by stacking vertically three unconnected thin metal plates [10]. This metal plates will have different desired patterns fabricated by chemical etching, creating a low-cost manufacturing product. This concept makes it possible to implement low loss and cost effective components such as bandpass, filter and directional couplers.

The metallic layers that compose the MLW do not require any electrical contact among them and are assembled allowing a small air gap among them, those avoiding complex manufacturing methods. Any field leakage do to the air gaps is prevented by using EBG structures around a transmission line fabricated by using chemical etching[11]. A basic design that exemplifies this concep can be found in Figure 2.14

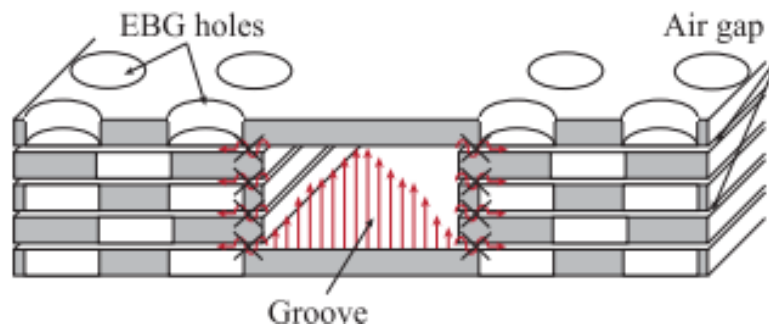


Figure 2.14: Cross-sectional view of an MLW transmission line with field-leakage suppression[11]

2.6 Antenna Theory

An antenna is an electronic device that converts energy from one form to another, in other words, a transducer for coupling electromagnetic energy between free space and a waveguide. It is the largest and most expensive structural part of a microwave system because it must have certain size due to physical limitations needed to satisfy and ensure the system operation.[2]

The way antennas work is by localizing the current in some region, creating a source for electromagnetic fields that propagate to far distances from the source[1]. In an isotropic antenna, this radiated waves are propagated in a spherical shape with the antenna at the center, and at large distances, the wave can be approximated as a plane wave. This plane wave will propagate according to the impedance of the medium, denoted as η , equal to 376.73Ω in free space.

As the waves propagate equally in all directions, the average power density decreases proportional to the growth ratio of the radiated sphere, which is R^2 . This ratio makes it important to be able to make an efficient usage of the power through the antenna design.

2.6.1 Antenna Parameters

The ability of the antenna to direct the input power into a particular direction is known as gain and is measured at the peak radiated intensity. Gain is closely related with directivity, it differs only by the efficiency, $Gain = Directivity \times efficiency$. [3].

In real applications, the power can't be completely radiated in the desired direction, and it creates side-lobes and back-lobes. This concepts are illustrated in figure 2.15.

Figure 2.15 is a plot showcasing the variation in intensity of an antenna, an isotropic antenna has no variation along all directions.

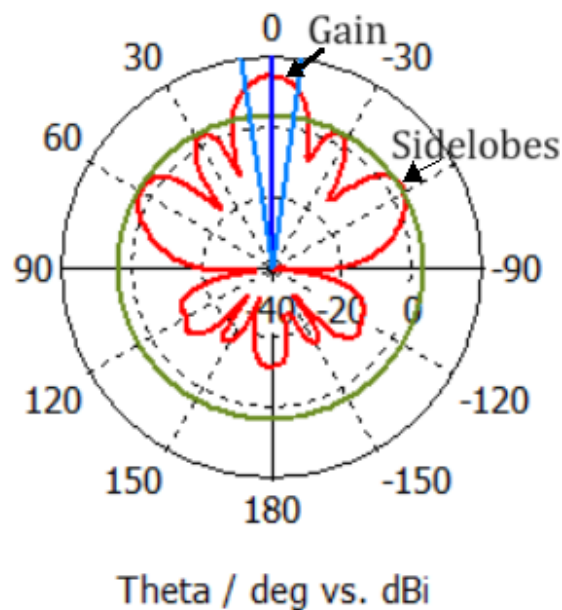


Figure 2.15: Polar plot of a radiation pattern, showing Gain and Side-lobes of an antenna (red) against the radiation pattern of an isotropic antenna (green)

2.6.2 Slot Antenna

There exist several type of antennas with their own specific applications, in cellular networks, and for frequencies around 68.5 GHz, a slot antenna presents different advantages. Slots are commonly desired antennas because they are cheap and accurate to manufacture [2].

Slot antennas are usually fed by waveguides with the advantage of using several slots to form a linear array, or by putting to lines side by side a two, dimensional array antenna[2].

Waveguide provide a rigid structure for the slots to couple to the internal fields travelling across the waveguide and controlling the amplitude of the slot excitation by the position and shape of the slot[3]. The fields excite the slot when this one interrupts the currents traveling along the waveguide walls [3], causing a voltage difference between the two sides of the slot, creating an electric field across the width of the slot, causing the radiation of the field. [3].

For the slot to radiate, it must have a resonant length near $\lambda/2$. This length depends on its geometry, the slot having a narrow width and thin waveguide walls. Waveguide slot arrays can produce can produce low sidelobe antennas with good efficiency, using the aperture of the slot and their distribution to determine the beam width and sidelobes.

Array antennas count with diverse advantages, from their geometry, they can be flat, making them more flexible for certain applications and for a better integration

in dynamic environments like automotive vehicles. It is also possible to control the shape of the beam by steering the phase of the signal and even achieve multiple beams in one same array[2].

3

Design

This chapter includes earlier work of the final design and a description of the base model under which the project is based.

The MLW Antenna proposed in this paper is based on MLW technology described in [10] in combination with the slot described in [4] to form a dual polarized slot antenna that works between the frequencies.

The first part of the design is to prepare a design for the waveguide as a coupled microstrip line to be able to take advantage of the two excitation modes described in chapter 2.3.2.

Once an approximation for the waveguide is designed, the following part is to design the slot based on the concept of the antenna element presented in [4]. And the last part is to implement it using MLW technology.

3.1 Waveguide Restrictions

According to the requirements of the system, the feeding system must support two different modes to be able to handle a dual polarized antenna without the necessity of two feeding systems. Using as a basis a coupled microstrip line, described in chapter 2.3.2 combined with gap waveguide technology (chapter 2.4) [4]. If coupling effects are ignored, the operation of the waveguide should be very similar to two separated waveguides. This waveguide should be able to excite the slot at the top of the design with two different polarizations.

When designing the waveguide, it is desired to use the gap waveguide technology as is easier to transfer a design from there into MLW, as done in [10]. To design the gap waveguide, it is important to define the desired way to feed it, following the proposed dual mode ridge gap waveguide in [4], inspired by the coupled microstrip line, it is possible to support odd and even mode in the same waveguide. To ensure a high isolation between the modes, the waveguide must be kept symmetrical throughout the antenna as explained in chapter 2.3.2. The first step is to design a coupled microstrip line that can support both desired modes along the waveguide as represented in figure 3.1.

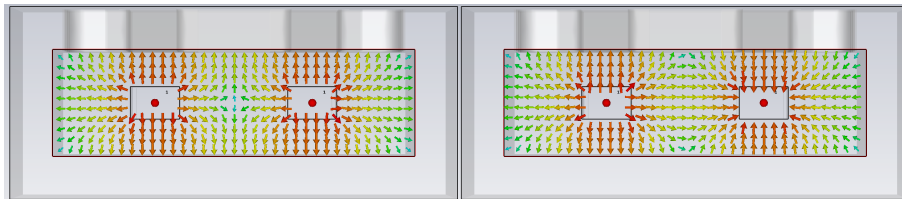


Figure 3.1: Even (left) and Odd (right) modes simulation in CST

Looking at figure 3.1 is easy to compare with figure 2.4, and assuming a distance big enough between the conductors and the walls, in a lossless dielectric, is possible to start with a first approximation of the dimensions required of the waveguide by making a theoretical analysis of the waveguide as a coupled microstrip line to work at a frequency of 68.5 GHz.

Starting with the size of the rectangular part of the waveguide for a wavelength of approximately $\lambda = 4.4mm$, the width should be at least $\lambda/2$, using physical limitations of constructing a plate with the etching technique in which Gapwaves has extensive experience, we can find some specifications in table 3.1 that can be used as a benchmark for the design of the coupled microstrip line sketched in figure 3.2.

Dimension	Expected Value
X	$\approx \lambda/2$
T	$> 0.15mm$
L	$0.15mm$
b	$< 0.8311mm$
W	$\ll X/2$
S	$\ll X$

Table 3.1: Specifications benchmark

The approximation for L comes from the paper on MLW [10], where the middle layer is designed with a height of $0.15mm$. The approximation for L , comes from a minimum distance desired between etched sections according to experimental background using this technique. The value for L comes from theoretical design of a rectangular waveguide that needs at least a width equal to half the wavelength of the desired frequency and for b an approximation of the height of a microstrip line using equation 3.1 were the W as shown in figure 2.3 is equal to $W = (\lambda/2)/2 = 1.2mm$ as two lines are required for the desired design, assuming an upper limit for having two lines that use all the width of the rectangular waveguide and an impedance of $\sqrt{\epsilon_r}Z_0 < 120\Omega$. [5]

$$\frac{W}{b} = x = \frac{30\pi}{\sqrt{\epsilon_r}Z_0} - 0.441 \quad (3.1)$$

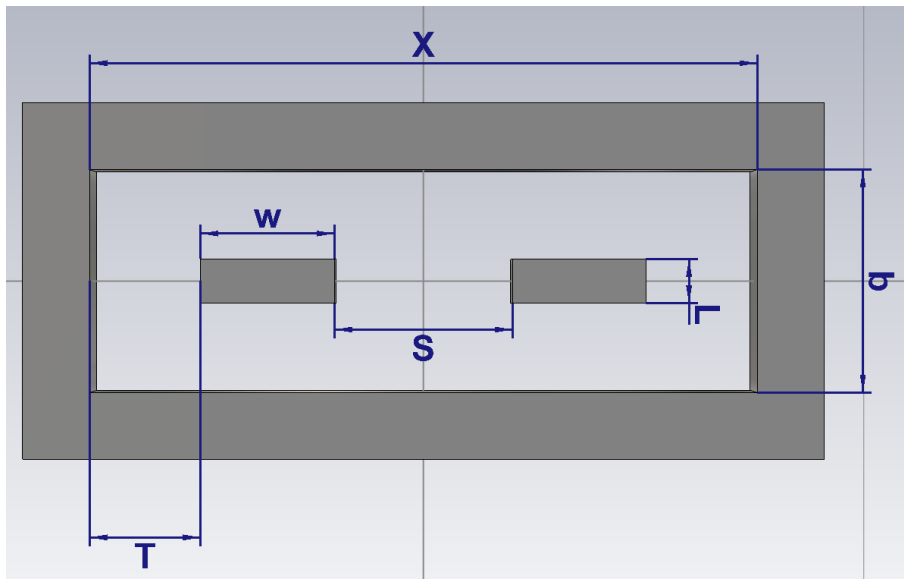


Figure 3.2: Dimensions nomenclature for the microstrip approximation

Usually the design of a coupled microstrip line, requires the use of a table as the one shown in figure 3.3, for this case it was approximated to impedance lower than 120Ω , to calculate the actual impedance, it would be necessary to know the equivalent network capacitance described in chapter 2.3.2. As this is a first approximation, and the network capacitance will change as the slot antenna is introduced the values will be changed and adjusted for MLW, a much broader approach is taken to get the upper limit of the dimensions on the waveguide.

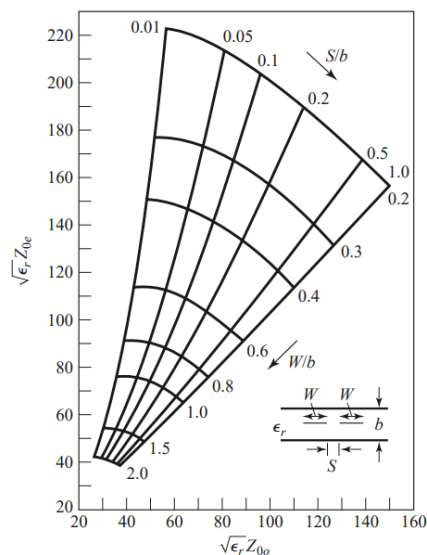


Figure 3.3: Normalized even- and odd-mode characteristic impedance design data for symmetric edge-coupled striplines [5]

3.1.1 Waveguide Design

With the limitations established, assuming an impedance $Z_0 \approx 50\Omega$ to decide the ratios of S/b and W/b with the upper limit obtained from equation 3.1. Through CST simulations, the ratios were approximated to be $W/b < 0.6$ and $S/b > 0.7$. Because of the proportional inverse relationship between W and S because of the restriction of maintaining the width of the waveguide $X \approx \frac{\lambda}{2}$.

The end of the waveguide is planned to be a short circuit, this will cause a reflection that in itself will cause a change of phase for both modes. This phase changes will cause undesired destructive interference that will affect the radiation efficiency of the slot antenna. To control this change is important to be aware of the distance of the short circuit to the slot, in figure 3.4 is plotted the distance in millimeters between the short circuit and the slot, portraying the change in the antenna efficiency for both modes. In order to have the best possible efficiency, it's is going to be necessary to adjust the distance to the short circuit separately for both modes, with focus on the first mode as it is the most sensible to the changes.

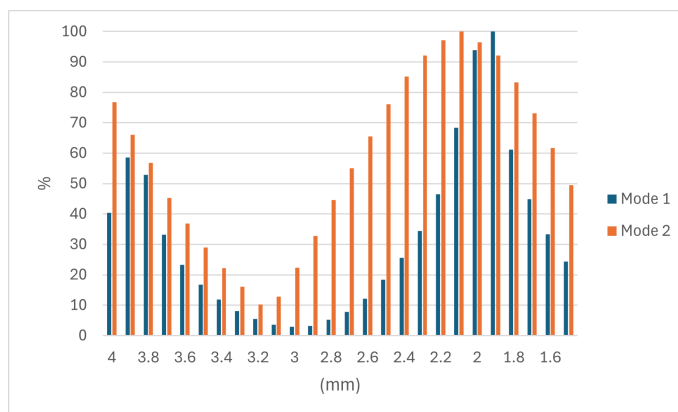


Figure 3.4: Transmission efficiency for each mode dependant of distance between the slot and the short circuit

3.2 MLW Restrictions

When adapting the model in MLW, The main limitations are the physical requirements of the layers. Aiming to maintain a model equal to the one proposed in [10], which consist on bottom and top layers with similar thickness ($400\mu m$) and a middle layer of $150\ 400\mu m$ as shown in figure 3.5.

As explained in 2.5, the objective of using MLW is to confine the wave using an EBG structure, from the results in the previous section, we have estimated values for the channel to be constructed around the inner conductor and the conductor size, to transfer the model to MLW is important to design the EBG structure for

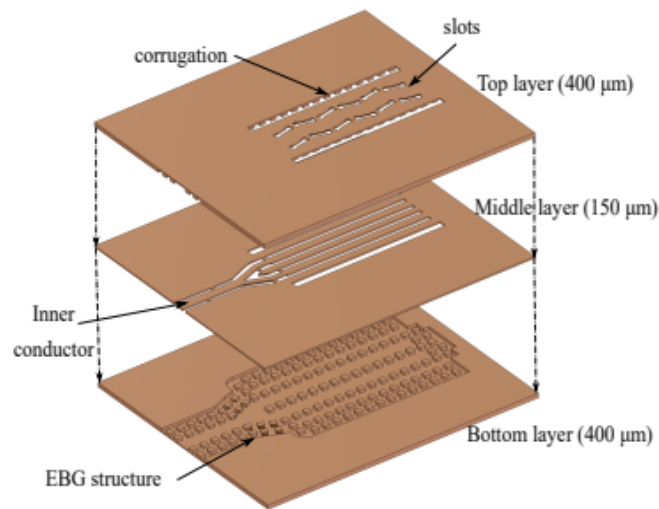


Figure 3.5: Expanded view of the MLW proposed in [10]

the desired frequency by selecting the size of the pins that constitute the structure.

3.2.1 Mode Selection

As explained in 2.4, the gap must be smaller than $\lambda/4$ to prevent leakage of the signal, with this physical constrain and to maintain symmetry, the size of each face was determined to start as $\text{Face} = \lambda/4 \approx 1.1\text{mm}$. Having the unit cell with the geometry shown in figure 3.6 as the base to verify for possible leakages and unwanted modes.

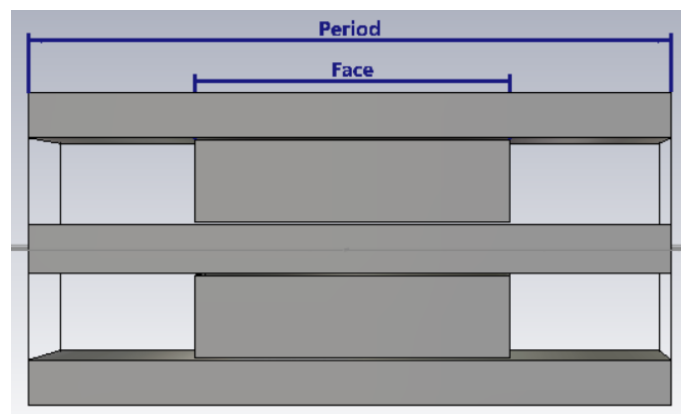


Figure 3.6: Geometry of the EBG unit cell

For the verification of the stopbands described in 2.4, the modes capable of leaking through the EBG structure are calculated for the unit cell using the CST Eigenmode solver, the resulting dispersion diagram is shown in figure 3.7.

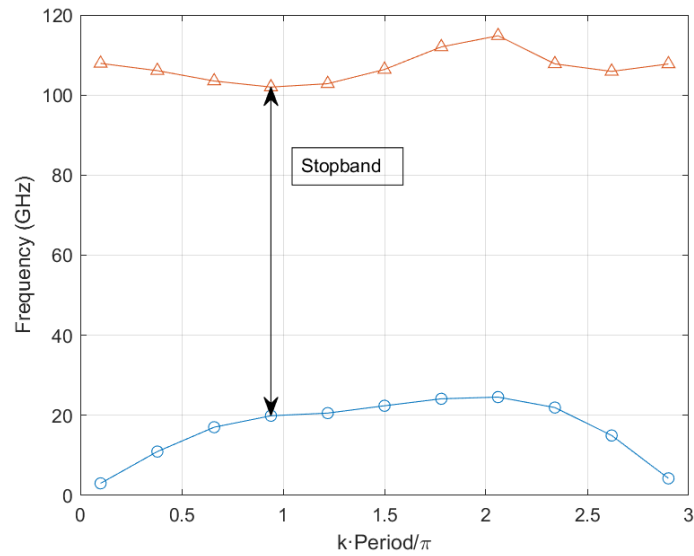


Figure 3.7: Dispersion diagram for the infinite periodic EBG unit cell ($Face = 1.1mm$, $Period = 2.2mm$)

To find how tight are the restrictions for the size of the faces of the pin, several simulations concerning the width of the pin, from $0.8mm$ to $1.2mm$ where done, the results are in figure 3.8 to show that is possible to change the size of the pin in case it is required.

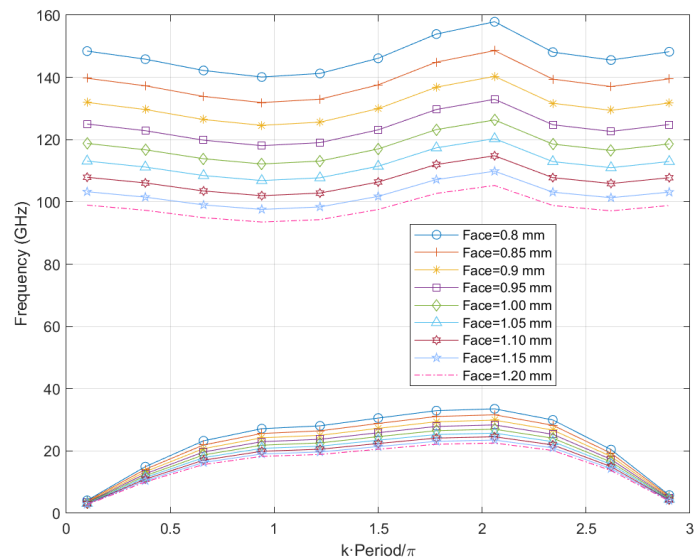


Figure 3.8: Dispersion diagram for the stopband of an infinite periodic EBG unit cell ranging from $Face = 0.8mm$, $Period = 1.6mm$ to $Face = 1.2mm$, $Period = 2.4mm$

To avoid undesired modes propagating through the waveguide, it is recommended to select the stopband closer to the desired bandwidth, this point will be expanded in the following section.

3.2.2 MLW Design

Once confirmed with the dispersion diagram that the desired bandwidth ($66\text{GHz} - 71\text{GHz}$) won't be leaked through the EBG structure, is possible to continue with the design and simulation of the whole waveguide to ensure that only the desired two modes will propagate without leakage. To ensure the propagation of the desired modes, is possible to simulate a transversal view of the waveguide as the one in figure 3.9 and use the CST Eigenmode solver to find the modes in the waveguide to ensure the correct functioning of the MLW.

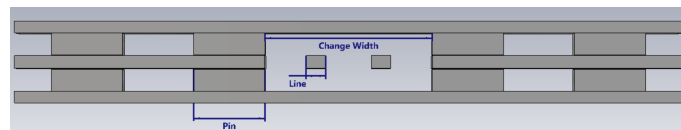


Figure 3.9: Transversal view of the waveguide

Using CST, the first 30 modes were simulated through the cross section to find the modes that propagate within the guide and ensure that there are only two propagating, this analysis is shown in figure 3.10.

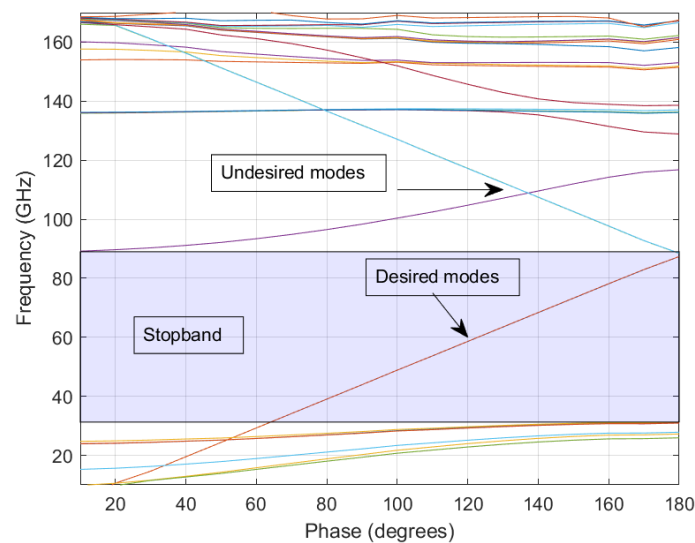


Figure 3.10: Dispersion diagram of the periodic transversal section of the MLW

After the first analysis, the size of the pin face was kept constant at 0.85mm and the width of the channel was swept from 1.5mm to 2mm to find the optimal width for the channel, the most significant modes are plotted in figure 3.11. While all the configurations keep the same two modes transmitting along the stopband, is possible to see the upper and lower level move dependant of the width of the channel. The desired width will be the closest one to the desired bandwidth to allow the biggest bandwidth to transmit without getting too close to the stopbands to avoid leakage of other modes.

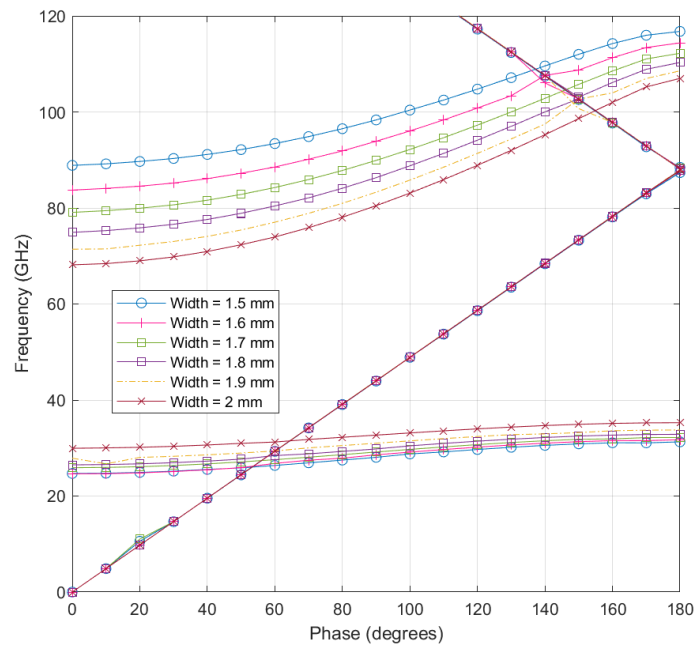


Figure 3.11: Dispersion diagram of the periodic transversal section of the MLW for different widths of the channel (1.5mm , 1.6mm , 1.7mm , 1.8mm , 1.9mm , 2mm)

3.3 Antenna Design

Using a single slot with two feeding lines will be capable of transmit only at one polarization according to it's position according to the propagation of the wave. In figure 3.12 is a depiction of two orthogonal slots that propagate two different linear polarizations feed by two feeding lines, odd or even mode.

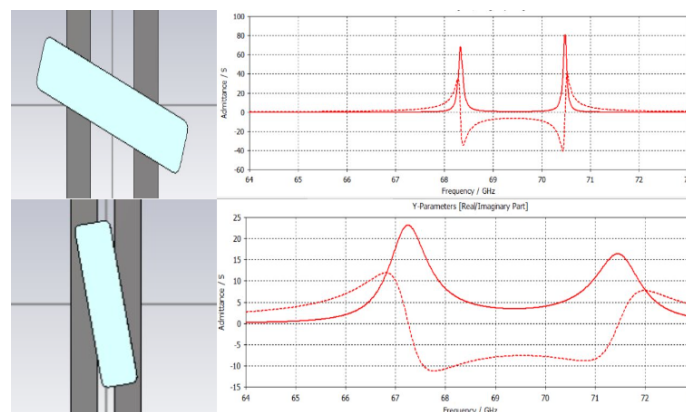


Figure 3.12: Admittance of the even mode (upper) and odd mode (lower) of a single slot

Parting from this two slots, is where the slot proposed in this project comes from, by adding both slots is proposed a slot with a "Y" form , as the one show in 3.13. Is also important to note that the single slot is tilted according to the transmission lines, this will be expanded in chapter 3.3.2

The design, is inspired by the concept presented in [4], and shown in figure 3.13, referred as tripole slots. In a traditional dual-polarized antenna, each polarization is fed by a different feeding system, this slot has a Y shape and is excited by the two modes traveling through the waveguide. Theoretically it can propagate two modes from the same slot, having the advantage of diminishing the quantity of slots required to work on both polarizations.

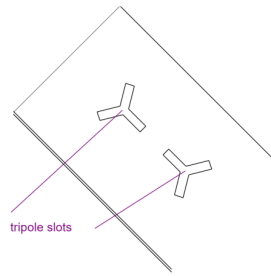


Figure 3.13: Schematic view of the antenna element tripole slots[4]

Starting analyzing the slot two different slots orthogonal to each other, as explained in [4], when placing the slot in the center of two feeding lines, only one of the slot will be excited in phase, the other lot will be excited out of phase and cancel out, a graphical depiction is shown in figure 3.14, the even mode can excite the vertical polarization, and the odd mode the horizontal one. The same principle applies when both slots are together as represented in figure 3.15, as long as the slot is symmetrical in the same way that the waveguide is, the modes will keep cancelling out ensuring high isolation between the modes and linear polarization as the result.

The slot can be analyzed as two different slots, if analyzed separated as shown in figure 3.14 is possible to recognize three main parameters that affect the excitation of the slot as width, angle between the upper arms, and length of as shown in figure 3.16.

The analysis of the slot will be done by observing the changes in admittance and resonant frequency, this will allow to understand its behaviour in terms of how the electromagnetic energy of both modes is radiated, and how its operational frequency is affected according to different changes. Starting with the width of the vertical slot shown in figure 3.16, is possible to plot the relative changes in frequency and admittance for both modes (figure 3.17).

According to the results plotted in 3.17, the vertical slot will have a higher impact on the odd mode frequency and admittance. In the opposite way, the width of the horizontal slot will have a higher impact on the even mode as shown in figure 3.18. It behaves similar to a normal slot, nevertheless, the width of either arm has an impact on both modes as it increases the length perception of the opposite slot. When analyzing the length, for the vertical slot, it has a direct impact on the odd

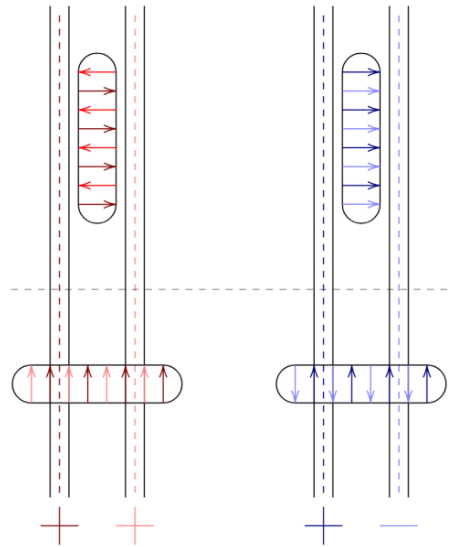


Figure 3.14: Excitation of the waveguide slots by the even mode on the left, and odd mode on the right[4]

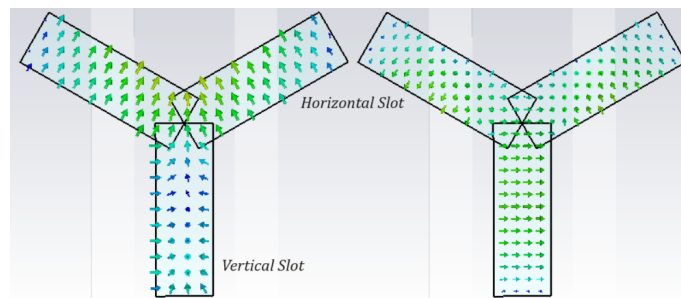


Figure 3.15: Excitation of the tripole slot with the even mode on the left, and odd mode on the right

mode and no impact on the even mode as seen in figure 3.19, but is not reciprocal with the length of the horizontal slot, as it impact mainly the even mode operation but also the odd mode as seen in figure 3.20.

The last parameter to analyze is the angle between the two upper arms. According to the results in figure 3.21, it has a higher impact on the Odd mode, specially in the admittance, but the effect that it has on the even mode is not negligible, the effect is similar for both modes, but most perceptible in the odd mode.

The three effects are also related between each other, meaning that depending on the angle, the width will affect the admittance of the mode in different magnitude.

Considering that the slot is going to be implemented in MLW, the biggest constrain for the slot is in the horizontal axis, in other words for the horizontal slot, the length will be fixed at $1.8mm$ as obtained from the design part in the chapter 3.2.1, this is an important limitation as in theory the slot needs to have a length of $\lambda/2 = 2.2mm$ for a central frequency of $68.5GHz$, but as seen from the behaviour of the slot, is

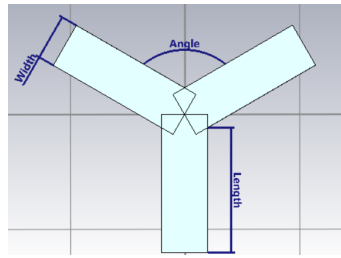


Figure 3.16: Main parameters for the tripole slot

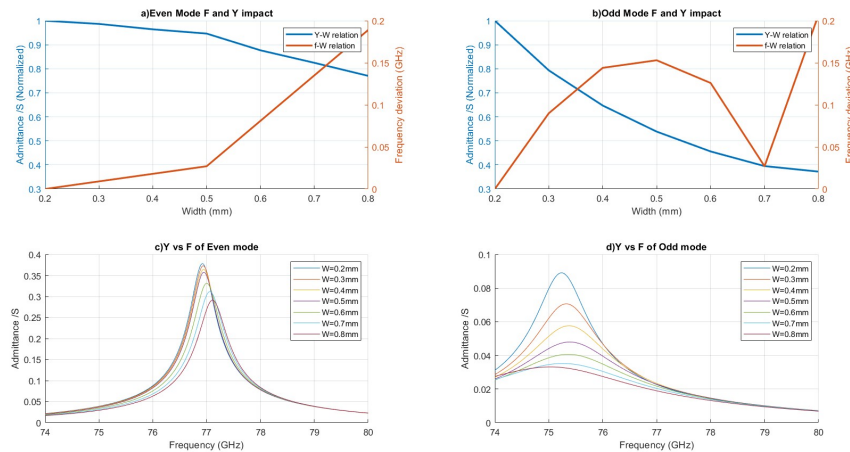


Figure 3.17: Effect of the Vertical slot Width on the Frequency and admittance
 a) Impact of Width Variation on Admittance and Frequency for the even mode
 b) Impact of Width Variation on Admittance and Frequency for the odd mode
 c) Admittance vs. Frequency of the even mode for Various Widths
 d) Admittance vs. Frequency of the odd mode for Various Widths

possible to adjust the frequency by changing the width, length and angle of the slot. For the vertical slot, it does not represent a big obstacle because the waveguide can extend vertically, in the same direction as the path along which the wave travels.

3.3.1 Extra Elements for the horizontal slot

To reach the desired operation frequency there were different iterations of the slot to try to find a simple option to increase the length of the horizontal slot and control in a more direct way the operational frequency, a variation of the slot with elements on the tips was researched, this model is shown in figure 3.22.

The idea behind this model is to research how the electrical length of the slot changes. Dumbbell shapes have been used to reduce the size of a slot antenna. Using these elements, it has been possible to reduce the final design size while maintaining a similar radiation performance [12]. This is due to the element extending the length of the slot and improving the surface current propagation, this is illustrated in figure

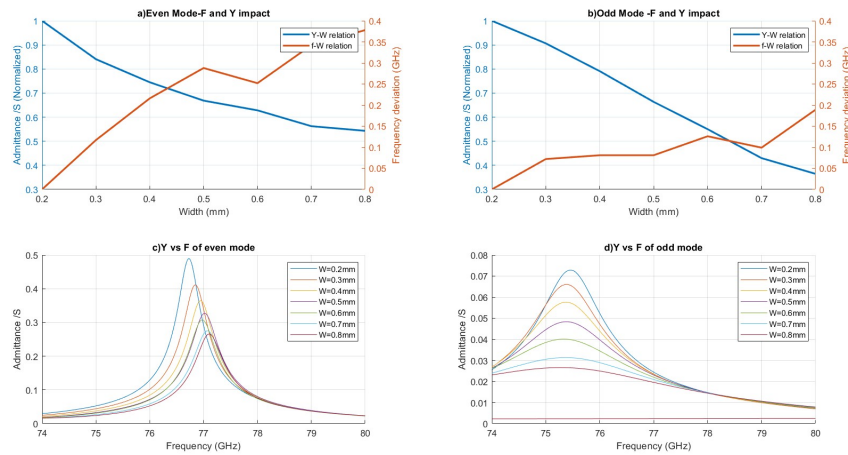


Figure 3.18: Effect of the Horizontal slot Width on the Frequency and admittance a) Impact of Width Variation on Admittance and Frequency for the even mode b) Impact of Width Variation on Admittance and Frequency for the odd mode c) Admittance vs. Frequency of the even mode for Various Widths d) Admittance vs. Frequency of the odd mode for Various Widths

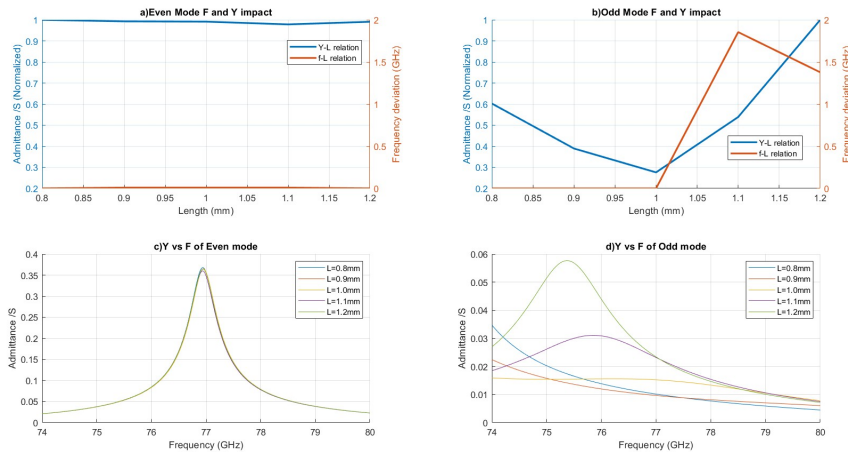


Figure 3.19: Effect of the Vertical slot Length on the Frequency and admittance a) Impact of Length Variation on Admittance and Frequency for the even mode b) Impact of Length Variation on Admittance and Frequency for the odd mode c) Admittance vs. Frequency of the even mode for Various Lengths d) Admittance vs. Frequency of the odd mode for Various Lengths

3.23. Is possible to observe the extended area that the E-field uses to propagate in the corners of the dumbbells.

The effect that this elements have in the reflection coefficient (S_{11}) of a short ended waveguide can be seen in figure 3.24, comparing two slots with the same dimensions and only difference in the presence of a $0.2mm$ dumbbell at the end of the horizontal slot.

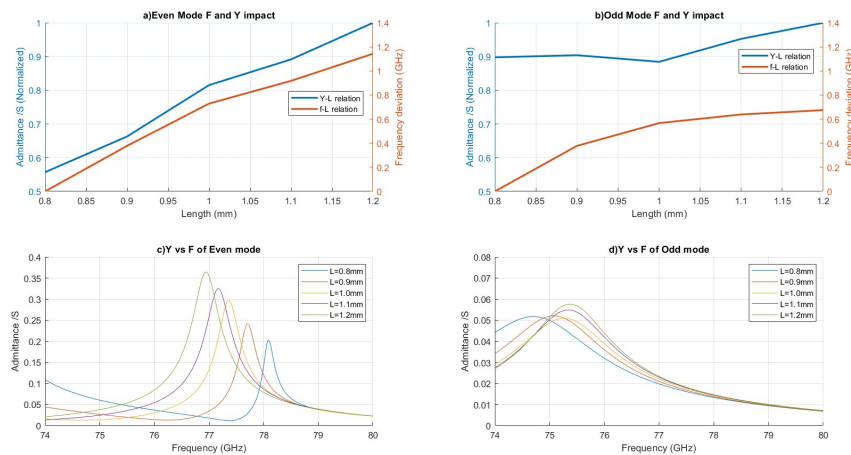


Figure 3.20: Effect of the Horizontal slot Length on the Frequency and admittance a) Impact of Length Variation on Admittance and Frequency for the even mode b) Impact of Length Variation on Admittance and Frequency for the odd mode c) Admittance vs. Frequency of the even mode for Various Lengths d) Admittance vs. Frequency of the odd mode for Various Lengths

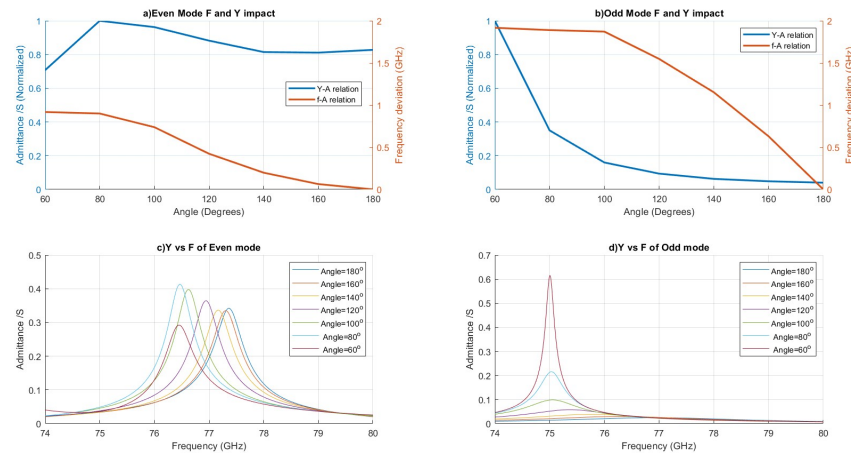


Figure 3.21: Effect of the Angle on the Frequency and admittance a) Impact of Angle Variation on Admittance and Frequency for the even mode b) Impact of Angle Variation on Admittance and Frequency for the odd mode c) Admittance vs. Frequency of the even mode for Various Angles d) Admittance vs. Frequency of the odd mode for Various Angles

The advantages depicted in figure 3.24 are as expected and detailed in [12], is possible to reach lower frequencies with the same length only adding the detailed element.

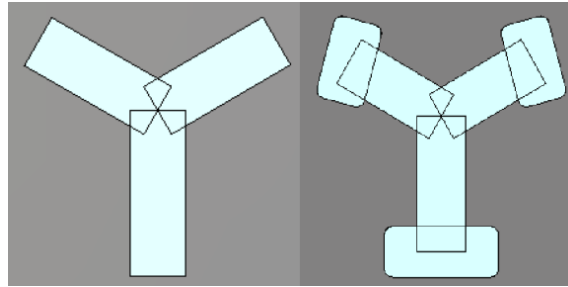


Figure 3.22: Initial Slot model on the left, and model with dumbbells on the right

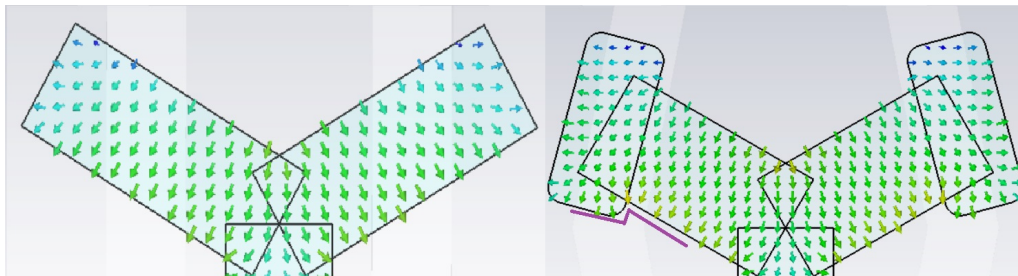


Figure 3.23: Electric field propagation in the horizontal slot, initial slot on the left, and slot with dumbbells on the right

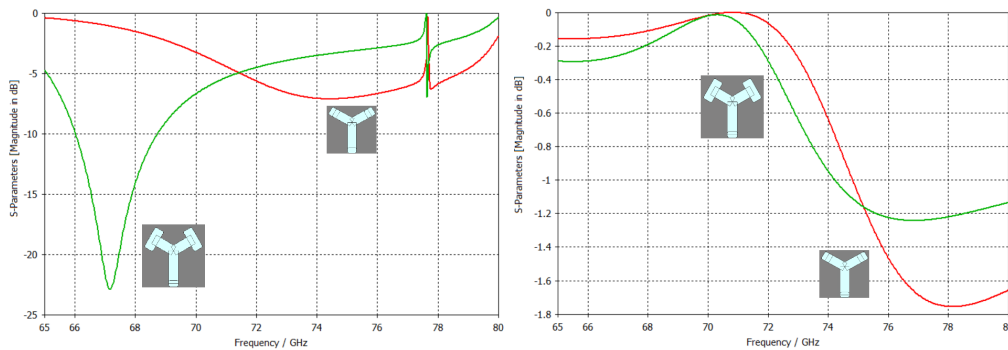


Figure 3.24: Comparison between the S_{11} parameter of the Even mode (left) and Odd mode (right), with 0.2mm dumbbells (green) and without (red)

3.3.2 Slot excitation

It is also important to take into account the direction of the feed lines, to achieve a better excitation of the slot, it was important to modify the inclination in which the lines were with respect to the slot as shown in the figure 3.25.

Bending the lines has a second effect making the electrical length of the line shorter than the distance between the slots. This has a direct effect on the phase of the signal at any distance between the slots, allowing also to have a better control of the grating lobes on the radiation pattern.

Focusing in the effect that the bent line has on the admittance of the slot, is possible to see the effects on figure 3.27, where the reflection coefficient S_{11} for both modes

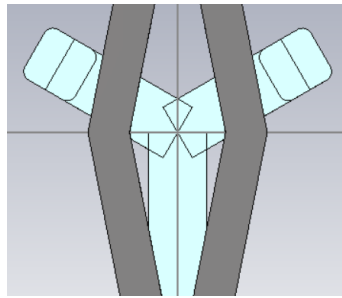


Figure 3.25: Feeding line bent to improve slot excitation

is plotted against the lines bent from 73° to 90° as shown in figure 3.26.

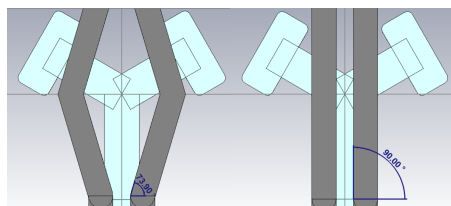


Figure 3.26: Feeding line bent comparison from 73° to 90°

Is possible to compare the effects caused by bending the line, as shown in figure 3.27, the effect in the reflection coefficient S_{11} has an opposite effect on the modes, but in terms of magnitude, it has a bigger effect on the even mode as it's the most sensible, but is the opposite for the frequency, where the odd mode is the most affected.

3.3.3 Horn

One of the objectives of this project is to study the grating lobes of the slot, for that, is possible to simulate an array of slots at an periodic distance to study the radiation pattern of the slot.

A simple element that can help to increase the directivity and decrease the side lobe level of a slot antenna, is a horn element on top of the slot. This element is well studied and known to improve the radiation pattern of antennas. As objective, it's set to achieve sidelobes lower than -10 dB.

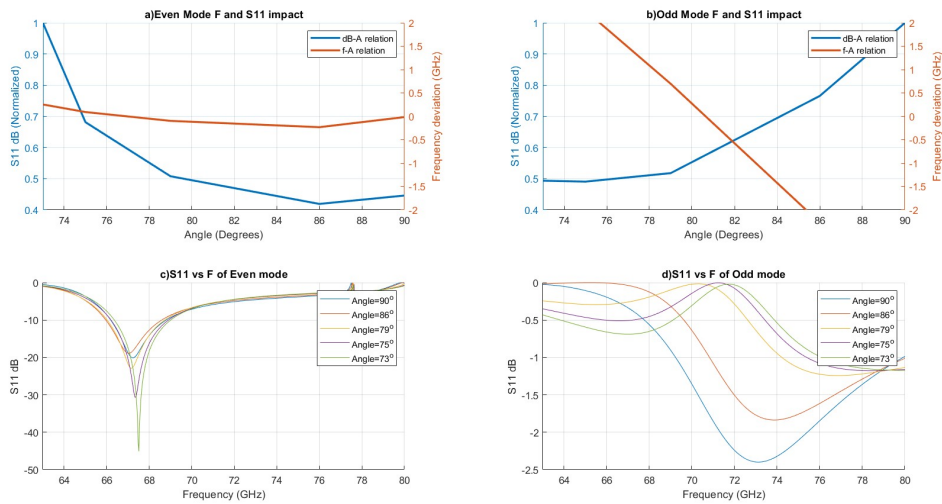


Figure 3.27: Effect of the Bent Lines on the Frequency and admittance a) Impact of Bent Lines on Admittance and Frequency for the even mode b) Impact of Bent Lines on Admittance and Frequency for the odd mode c) Admittance vs. Frequency of the even mode for Various Lengths d) Admittance vs. Frequency of the odd mode for Various Lengths

4

Results

The results presented in this chapter are presented in the same order as the chapter 3 is set, starting from the waveguide and follow by the final slot design.

4.1 MLW Results

Starting with the design restrictions explained in 3.1, the lines dimensions depend on b (figure 3.2). To define it's value using the proposed values in the MLW paper [10] were $b \approx 0.7mm$. This allows to have better approximations for the rest of the dimensions. The lines should have a width smaller than $0.42mm$, according to $W/b < 0.6$ while staying at a distance bigger than $0.48mm$ according to $S/b > 0.7$.

The width of the channel will be selected when designing the MLW, as explained in chapter 3.2 the biggest constrain for the multi-layer waveguide, is for the stop bands to allow only 2 modes to propagate, as shown in figure 3.8, the considered pin sizes will work for any size between $0.8mm$ and $1.2mm$ as these are values smaller than $\lambda/4$. The next part is for the width of the channel to allow only two modes. As expressed in figure 3.11, the width of the channel should be kept around $1.8mm$ to avoid unwanted modes to leak into the channel. This will result in an initial schematic as shown in figure 4.1.

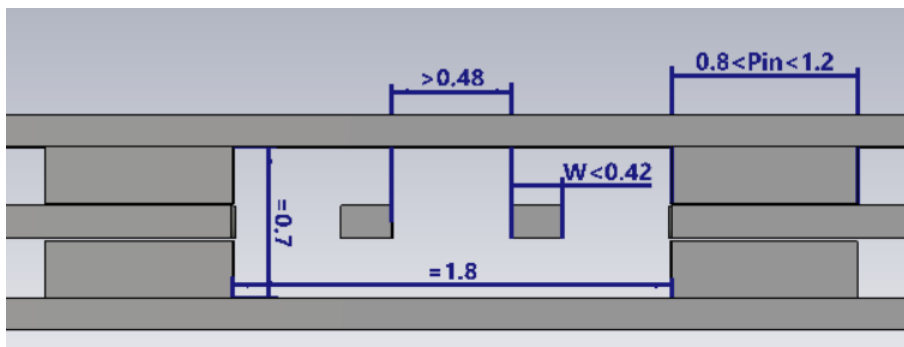


Figure 4.1: Approximated dimensions for the MLW design

The rest of the dimensions of the MLW will follow the design proposed in [10] and in chapter 3.2.

As a result of the channel dimensions, when designing the slot, the biggest constrain is the length of the horizontal line. The bending on the lines will maintain their distance between the indicated range.

4.2 Slot results

Although the results obtained with the dumbbells were promising, the physical implementation results problematic. The dumbbells area reduce the distance between the aperture and the pins, as shown in figure 4.2. This distance should be bigger than $0.2mm$ according to experimental data from different projects elaborated at Gapwaves, but the dumbbells were located at least $0.15mm$ from a pin, and this will cause collision or overlap when implemented

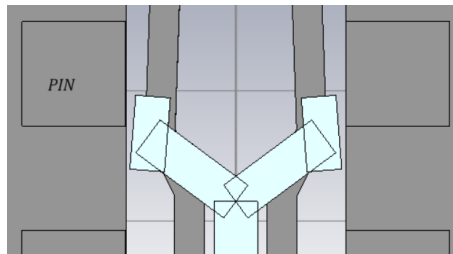


Figure 4.2: Slot design with dumbbells delimited by proximity to the side pins

To reach the desired operating frequency, two small wings in between the pins were added to the end of the horizontal slot to be able to extend it's resonant frequency. In order to do this, the size and periodicity of the pins was adjusted to $1mm$ and $2mm$ respectively fulfilling the size expectations delimited in 4.1. This pin size allows for the horizontal slot to extend in between them with a width of $0.4mm$. For the vertical slot, there were no constrains to fulfil, so no extra element was added. The final slot is in figure 4.3.

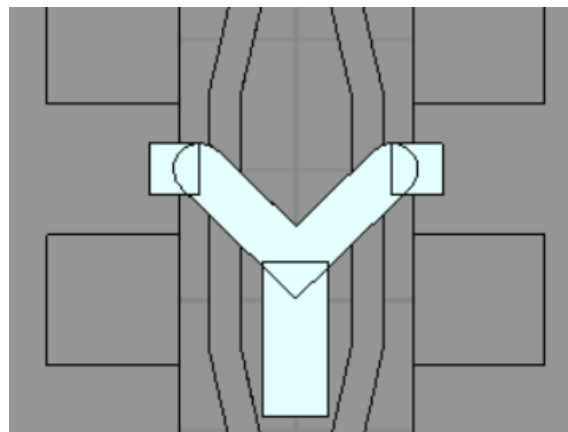


Figure 4.3: Final slot design

Regarding the lines, the best configuration is the shown in figure 4.3, the distance between the two lines are kept bigger than $0.48mm$, at the closer point they are at $0.48mm$ and at their furthest point at $0.85mm$, respecting a minimum distance of $0.2mm$.

For the final slot dimensions, the focus is in propagating the even mode through the horizontal slot as it is the limited by the waveguide width. As the length of the horizontal slot is already limited and is dependant on the angle, the width is limited to be at the maximum possible value of $0.4mm$ (due to the pin size). The next parameter to select is the angle, as seen in figure 3.21 c), smaller angles direct to lower frequencies and higher admittance for the even mode. The rest of the dimensions are initially chosen from the best values in chapter 3.3, and optimized for the best operational parameters for the slot. The final dimensions are shown in figure 4.4.

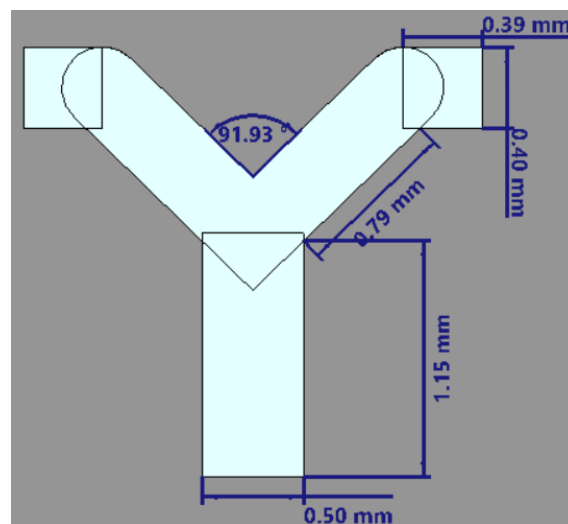


Figure 4.4: Dimensions of the final slot

4.3 Operation

The result S_{11} parameters obtained from the design described in the last two sections are in figure 4.5 for the even mode, and 4.6 for the odd mode in a 3 slot array antenna.

For the radiation pattern, it was necessary to implement a horn section to lower the sidelobes and improve the antenna directivity. The comparison of radiation pattern of the unit antenna with and without horn are in figure 4.7 for the odd mode, and in figure 4.8 for the Odd mode.

Implementing three slots as seen in figure 4.9, the radiation pattern of the even mode is depicted in figure 4.10. The radiation pattern of the odd mode is depicted in figure 4.11.

4. Results

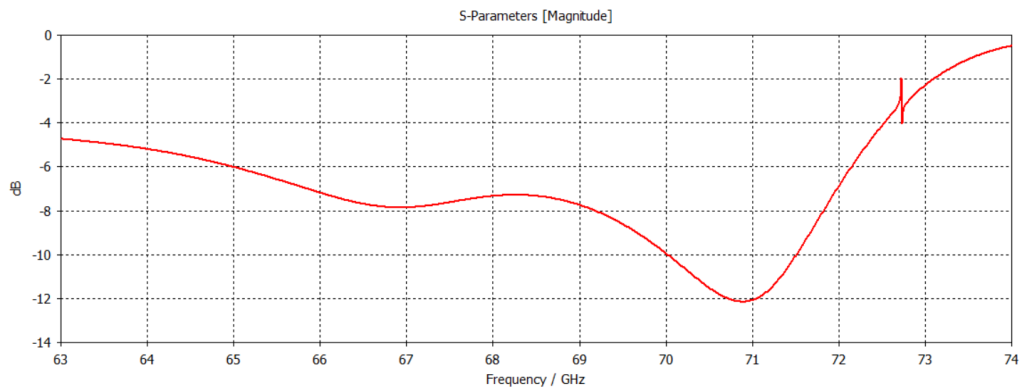


Figure 4.5: S_{11} Parameter Against Frequency of the even mode

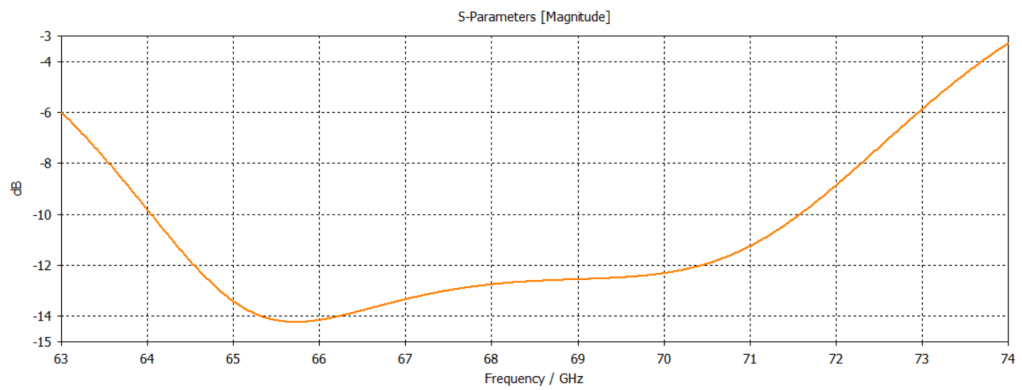


Figure 4.6: S_{11} Parameter Against Frequency of the even mode

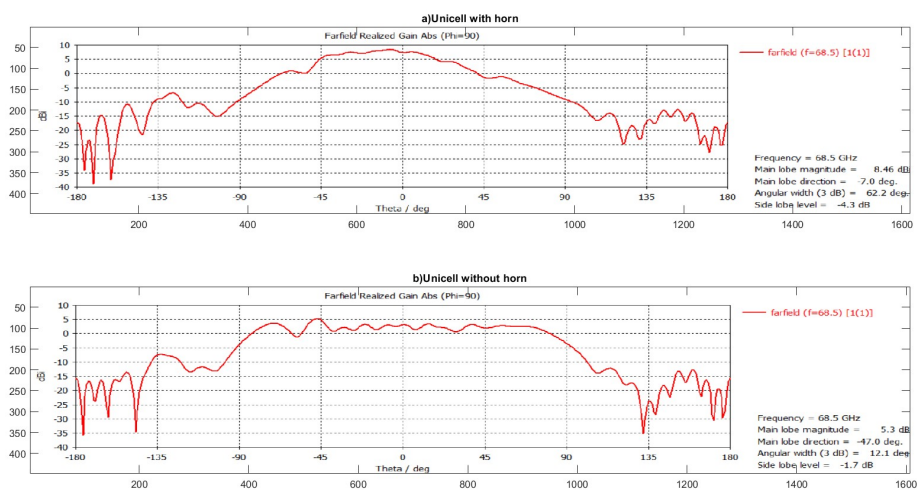


Figure 4.7: Even mode Elevation Radiation pattern of one slot antenna a) With Horn b) Without Horn

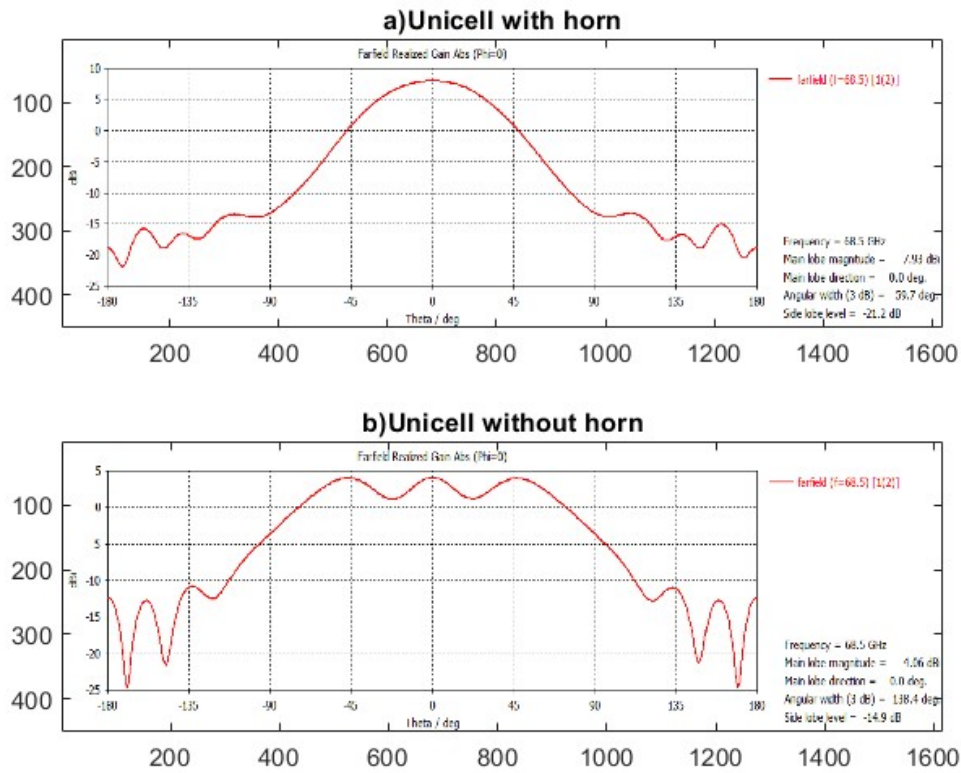


Figure 4.8: Odd mode Azimuth Radiation pattern of one slot antenna a) With Horn b) Without Horn

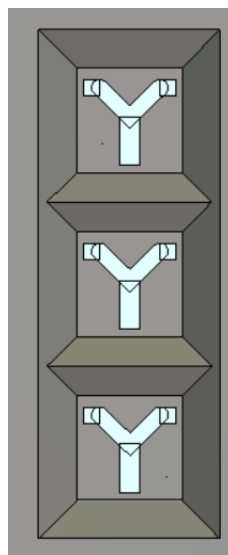


Figure 4.9: 3 Slots model

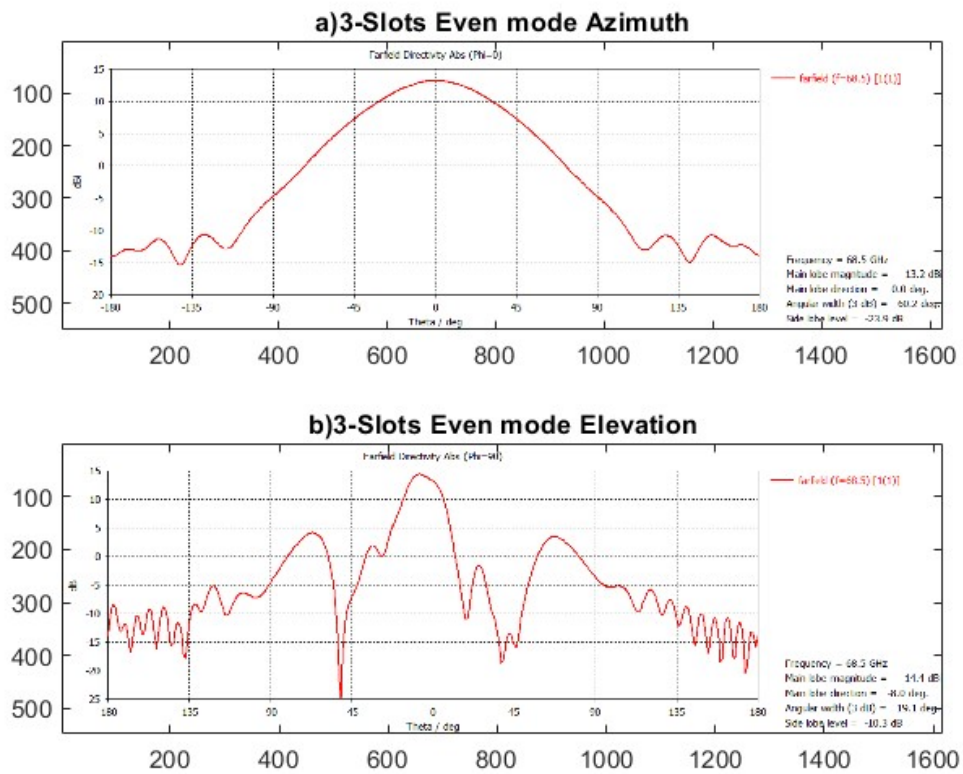


Figure 4.10: Even mode Radiation pattern of three slots with horn a)Azimuth
 b)Elevation

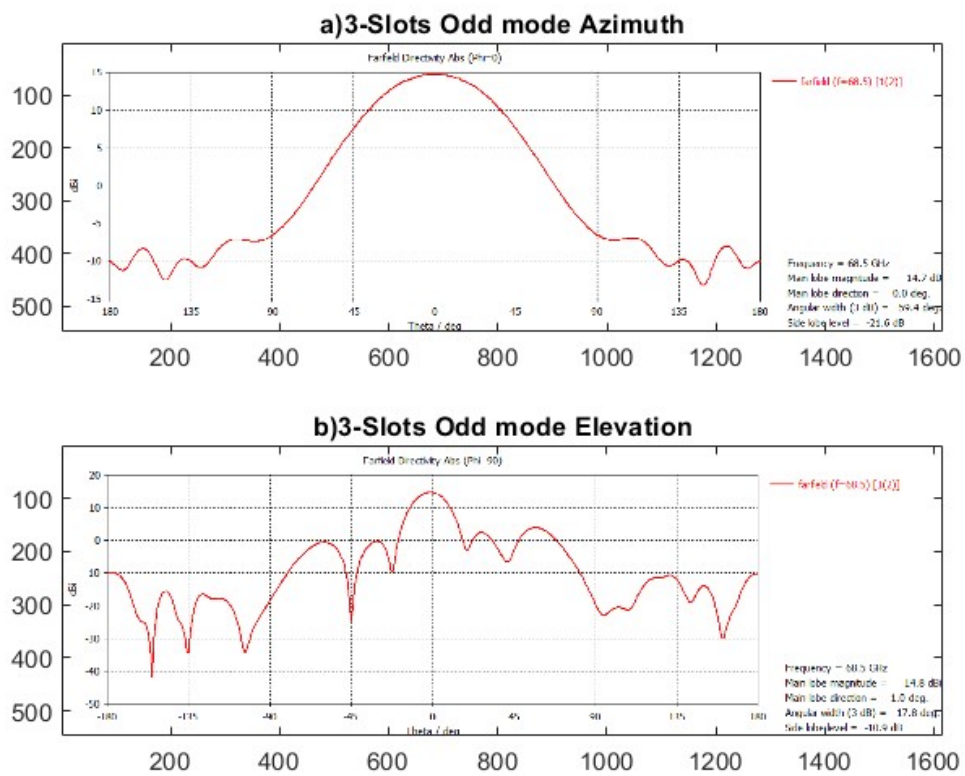


Figure 4.11: Odd mode Radiation pattern of three slots with horn a)Azimuth
b)Elevation

5

Discussion

In this chapter I review the results obtained and the process to conclude the viability and impact of the proposed antenna.

5.1 Performance

Starting with the reflection coefficient plotted in figure 4.5 and 4.6, It was possible to achieve the desired bandwidth from $66GHz$ to $71GHz$. As expected, the odd mode has a better reflection coefficient, meaning a better transmission, this is due to the slot having more space to increase its length, and comparing to the result of the even mode, it's clear the disadvantage of being constrained by the waveguide width.

About the radiation pattern, the most important detailed is the comparison between azimuth and elevation, elevation being the direction with the highest distortion on envelope. Comparing figure 4.7 with figure 4.8, there is a clear discrepancy in the pattern, where the even mode is mostly offset. The difference in direction is still noticeable when the horn is implemented, but it decrease down to 7° .

About the sidelobes, they are more noticeable in the elevation axis, and the presence of more slots help to decrease their effect, because of this, it would be recommended to implement with at least 3 slots. This is backup by the S_{11} results, where it was needed three slots to achieve $-10dB$ for the odd mode and $-6dB$ for the even mode. It's also important to mention that with the lines configuration, the slots were located at $4.04mm$, or 0.9λ .

The improvement that the horn and having multiple slots (3) has on the radiation pattern is noticeable in figures 4.11 and 4.10, where the sidelobes for both modes are lower than $-10dB$, nevertheless, the direction of the even mode remains with an offset.

5.2 Slot

In concordance with chapter 3, the characterization of the antenna is important be able to understand its behavior, and the trade offs that remain between the even and odd mode admittance, specially in the designing of the slot, the angle, and to

keep in mind that one of the mods will be constrained by the desired frequency. The designing steps in chapter 3 offer a preliminary threshold and what to expect when designing the proposed antenna, specially to avoid measurements passing an acceptable trade off either in operational frequency or admittance.

This slot shows highly promising results in adaptability and flexibility to be used to transmit in two polarizations. The main difficulties consist on exciting the slot in an optimum way and having enough space on the layer to be implemented on MLW.

5.3 Future work

Although the slot behavior is well documented and characterized, the impact magnitude that some parameters have in the slot, depend on the value of others (like the angle and width of the slot). An interesting study to make is to evaluate the impact that each parameter has over the impact of a second parameter.

A future physical model is pending to corroborate the functionality of the slot antenna, as well it's physical integration using MLW technology in a turbulent environment.

The model still offers room of improvement, due to the location of the horizontal slot, there is a mismatch in it's position in comparison with the vertical slot. By improving the horn to take into account this mismatch, it should be possible to improve the direction of the main lobe.

A study at different frequencies with different bandwidths could find new possible applications for this dual polarized antenna, for example radar.

5.4 Conclusion

As final thoughts, the dipole slot presents a good opportunity to improve the spectral efficiency in the mmWave regime, while being capable to be implemented in MLW. The biggest constrain will remain being the horizontal slot. Is possible to achieve more satisfactory results depending of the requirements, having a smaller bandwidth would improve the achievable reflection coefficient of the even mode.

Bibliography

- [1] Sophocles J. Orfanidis. (2016) *Electromagnetic Waves and Antennas*. 94 Brett Road Piscataway, NJ: Rutgers University, 2016.
- [2] Per-Simon Kildal. *Foundations of Antenna Engineering : A Unified Approach for Line-of-Sight and Multipath*. Sweden, Chalmers University of Technology, 15 Mar. 2021.
- [3] Milligan, T. A. (2005). *Modern antenna design (Second)*. IEEE Press.
- [4] Van de Ven, Coen. *Concept and Design of a 1-D Scanning Dual Polarized Antenna Element in Gapwaveguide Technology*. 28 June 2021.
- [5] Pozar, D. M. (2021). *Microwave engineering (Fourth)*. Wiley India.
- [6] Transverse Electro-Magnetic (TEM). (n.d.). [Www.microwaves101.com](http://www.microwaves101.com). Retrieved May 20, 2024, from <https://www.microwaves101.com/encyclopedias/transverse-electro-magnetic>
- [7] Per-Simon Kildal, et al. "Design and Experimental Verification of Ridge Gap Waveguide in Bed of Nails for Parallel-Plate Mode Suppression." *Iet Microwaves Antennas & Propagation*, vol. 5, no. 3, 17 Feb. 2011, pp. 262–262, <https://doi.org/10.1049/iet-map.2010.0089>. Accessed 21 Apr. 2023.
- [8] Y. Komatsu and Y. Murakami, "Coupling Coefficient Between Microstrip Line and Dielectric Resonator," *IEEE Transactions on Microwave Theory and Techniques*, vol. MTT-31, pp. 34–40, January 1983.
- [9] Zhi Ning Chen, et al. *Handbook of Antenna Technologies*. Singapore, Springer Reference, 2016.
- [10] Abbas Vosoogh, et al. *Novel Low-Loss Coaxial Slot Array Based on Gap Waveguide Technology for E-Band Automotive Radar Applications*. 26 Mar. 2023, <https://doi.org/10.23919/eucap57121.2023.10133242>. Accessed 24 May 2024.
- [11] A. Vosoogh, H. Zirath, and Z. S. He, "Novel air-filled waveguide transmission line based on multilayer thin metal plates," *IEEE Transactions on Terahertz Science and Technology*, vol. 9, no. 3, pp. 282–290, 2019
- [12] Karmokar, Debabrata K., and Shu-Lin Chen. "Slot Antenna Miniaturization by Loading Dumbbell-Shaped Slots and Strips, Square-Shaped Loops, and Shorting Vias." *Microwave and Optical Technology Letters*, vol. 62, no. 6, June 2020, pp. 2307–2310, <https://doi.org/10.1002/mop.32312>. Accessed 20 May 2022.

DEPARTMENT OF SOME SUBJECT OR TECHNOLOGY
CHALMERS UNIVERSITY OF TECHNOLOGY
Gothenburg, Sweden
www.chalmers.se



CHALMERS
UNIVERSITY OF TECHNOLOGY